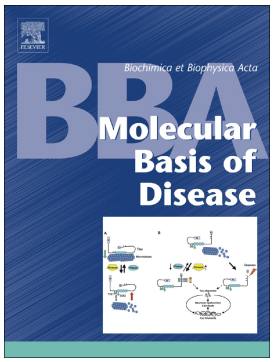


# Blood-brain barrier dysfunction underlying Alzheimer's disease is induced by an SSAO/VAP-1-dependent cerebrovascular activation with enhanced Aβ deposition

Montse Solé, María Esteban-Lopez, Biel Taltavull, Cristina Fábregas, Rut Fadó, Núria Casals, Jose Rodríguez-Álvarez, Alfredo J. Miñano-Molina, Mercedes Unzeta

PII: S0925-4439(19)30144-9
DOI: https://doi.org/10.1016/j.bbadis.2019.04.016
Reference: BBADIS 65460

To appear in: *BBA - Molecular Basis of Disease*

Received date: 20 November 2018
Revised date: 3 March 2019
Accepted date: 26 April 2019

Please cite this article as: M. Solé, M. Esteban-Lopez, B. Taltavull, et al., Blood-brain barrier dysfunction underlying Alzheimer's disease is induced by an SSAO/VAP-1-dependent cerebrovascular activation with enhanced Aβ deposition, BBA - Molecular Basis of Disease, https://doi.org/10.1016/j.bbadis.2019.04.016

**Blood-brain barrier dysfunction underlying Alzheimer's disease is induced by an SSAO/VAP-1-dependent cerebrovascular activation with enhanced Aβ deposition**

Montse Solé[a*1], María Esteban-Lopez[a], Biel Taltavull[a], Cristina Fábregas[a], Rut Fadó[b], Núria Casals[b,c], Jose Rodríguez-Álvarez[a,d,e], Alfredo J. Miñano-Molina[a,d] and Mercedes Unzeta[a*]

[a]*Biochemistry and Molecular Biology Department. Institute of Neurosciences (INc). Universitat Autònoma de Barcelona (UAB), Bellaterra (Barcelona), Spain.*

[b]*Basic Sciences Department, Facultat de Medicina i Ciències de la Salut, Universitat Internacional de Catalunya (UIC), Sant Cugat del Vallès, Spain.*

[c]*Centro de Investigación Biomédica en Red de Fisiopatología de la Obesidad y la Nutrición (CIBEROBN), Santiago de Compostela, Spain.*

[d]*Centro de Investigación Biomédica en Red sobre Enfermedades Neurodegenerativas (CIBERNED), Madrid, Spain.*

[e]*Dominick P. Purpura Department of Neuroscience, Albert Einstein College of Medicine, New York, NY 10461, USA.*

***Corresponding authors:** Montse Solé and Mercedes Unzeta, Biochemistry and Molecular Biology Department, Institute of Neurosciences, Universitat Autònoma de Barcelona. 08193 Bellaterra (Barcelona), Spain. Tel: +34 93 581 1624; Emails: spmontse2@gmail.com; mercedes.unzeta@uab.es

[1]Present address: Neurovascular Research Laboratory, Vall d'Hebron Research Institute, Universitat Autònoma de Barcelona. Passeig Vall d'Hebron, 119-129, 08035 Barcelona, Spain. Tel: +34 93 489 4399.

**Running title:** SSAO/VAP-1 activates brain endothelium

**Abstract**

Dysfunctions of the vascular system directly contribute to the onset and progression of Alzheimer's disease (AD). The blood-brain barrier (BBB) shows signs of malfunction at early stages of the disease. When Abeta peptide (Aβ) is deposited on brain vessels, it induces vascular degeneration by producing reactive oxygen species and promoting inflammation. These molecular processes are also related to an excessive SSAO/VAP-1 (semicarbazide-sensitive amine oxidase) enzymatic activity, observed in plasma and in cerebrovascular tissue of AD patients. We studied the contribution of vascular SSAO/VAP-1 to the BBB dysfunction in AD using *in vitro* BBB models. Our results show that SSAO/VAP-1 expression is associated to endothelial activation by altering the release of pro-inflammatory and pro-angiogenic angioneurins, most highly IL-6, IL8 and VEGF. It is also related to a BBB structure alteration, with a decrease in tight-junction proteins such as zona occludens or claudin-5. Moreover, the BBB function reveals increased permeability and leukocyte adhesion in cells expressing SSAO/VAP-1, as well as an enhancement of the vascular Aβ deposition induced by mechanisms both dependent and independent of the enzymatic activity of SSAO/VAP-1. These results reveal an interesting role of vascular SSAO/VAP-1 in BBB dysfunction related to AD progression, opening a new window in the search of alternative therapeutic targets for fighting AD.

**Keywords:** Alzheimer's disease (AD), angioneurins, blood-brain barrier (BBB), neurovascular unit (NVU), semicarbazide-sensitive amine oxidase (SSAO/VAP-1).

## 1. Introduction

Besides the two main pathological hallmarks of Alzheimer´s disease (AD), which include extraneuronal β-amyloid (Aβ) plaques and neurofibrillary tangles, other traits are also present in AD, such as cerebral amyloid angiopathy (CAA), inflammation and cerebral hypoperfusion. Literature supports nowadays that the cerebrovasculature importantly contributes to the onset and progression of AD [1-6], postulating the existence of a strong link between vascular damage and this pathology. This link is evidenced for instance, by the fact that a high percentage of patients having suffered stroke subsequently develop AD [7], or by the increased blood-brain barrier (BBB) permeability found in mild cognitive impairment (MCI) patients [8].

Hypoperfusion/hypoxia is thought to play an important role in AD pathogenesis [9], as being responsible of vascular activation [2] and angiogenesis induction [10]. Factors responsible of angiogenesis are found upregulated in brain microvessels of AD patients [11] and in transgenic mouse models of AD [12]. However, despite the pro-angiogenic factors release observed in the AD brain, they are not correlated with increased vascularity. Therefore, no shut off feedback signals are generated, and endothelial cells become irreversibly activated [2]. AD microvessels release a wide variety of bioactive, neurotoxic and inflammatory factors promoting vascular activation and angiogenesis, including interleukins, tumor necrosis factor alpha (TNF-α), vascular endothelial growth factor (VEGF) and matrix metalloproteinases (MMPs) [2,13]. These mediators are known as angioneurins, a terminus including angiogenic factors released at the nervous system as well as neurotrophic factors with angiogenic properties [14]. Their release has deleterious consequences for the neuronal health and brain homeostasis, affecting the neurovascular unit (NVU) function [15]. The NVU, integrated by neurons, astrocytes, brain endothelium, pericytes, vascular smooth muscle cells and microglia, constitutes a functional unit able to maintain the homeostasis of the brain's microenvironment, controlling the exchange of molecules across the BBB, regulating blood flow, supplying trophic support and maintaining the immune surveillance of brain cells [16]. Therefore, the study of neurovascular crosstalk and its alterations is important to understand the molecular basis of AD.

BBB dysfunction associated to the AD pathogenesis has been shown in transgenic mouse models, in which BBB integrity is already compromised before developing amyloid plaques and

cognitive impairment [17,18]. Oxidative stress is also increased in brain blood vessels in the APP23 mouse model before the emergence of amyloid plaques or CAA [19], which may contribute to this loss of the BBB integrity, but also to the vascular activation itself. Among different reactive oxygen species, hydrogen peroxide ($H_2O_2$) is one of the most important endothelium-derived modulators of vascular function involved in the AD pathophysiology, as it is able to interact with multiple signaling systems [20]. In the same line, the BBB in AD seems to be more vulnerable to inflammation, becoming leaky in AD brains of transgenic mouse models and therefore allowing peripheral inflammation spreading into the brain [21]. Thus, a cerebrovascular system dysfunction displaying angioneurins release, oxidative stress, inflammation and BBB leakage seems to be strongly related with the AD pathogenesis, and prompts to a pharmacological intervention aimed to reduce vascular activation in order to improve cognitive function underlying this pathology [15,22]. However, the molecular mechanisms responsible of these vascular alterations, and therefore, the potential therapeutic targets, are still not well established.

In this regard, the increased overexpression of the vascular-adhesion protein (VAP-1), a homodimeric glycoprotein with semicarbazide-sensitive amine oxidase (SSAO, E.C 1.4.3.21) enzymatic activity, found in cerebrovascular tissue of AD patients, may turn it into a good candidate.

SSAO/VAP-1 appears overexpressed in cerebrovasculature from AD patients [23], and released into blood plasma in AD [24], cerebral ischemia [25-27] and other pathologies displaying inflammation [28-30]. As an enzyme, it generates $H_2O_2$, aldehydes and ammonia as metabolic products, which are able to induce cellular damage when overproduced [31,32], but it is also able to modulate the expression of other adhesion molecules [33,34] and to enhance Aβ aggregation [35,36]. SSAO/VAP-1 behaves also as an adhesion protein, binding leukocytes through its enzymatic activity [37,38], and allowing their infiltration through the BBB into the brain parenchyma, enhancing cell damage and brain inflammation. Therefore, it is believed that the increased SSAO/VAP-1 levels may contribute to the physiopathology of these diseases, and specifically of AD.

In the context of AD pathology, the main objectives of this study were to assess whether the overexpression and/or activity of SSAO/VAP-1 in human microvascular brain endothelial cells are involved in endothelial activation, through the modification of angioneurins release, altering the BBB function, hence elucidating the role of SSAO/VAP-1 in the BBB dysfunction. Furthermore, we decided to confirm whether SSAO/VAP-1 is able to modify vascular Aβ deposition, altering BBB permeability and leukocyte adhesion using a NVU experimental model.

## 2. Materials and methods

If not otherwise indicated, reagents were purchased from Sigma Aldrich, Madrid, Spain.

### 2.1. Cell lines

The hCMEC/D3 cell line (human cerebral microvascular endothelial cells) was obtained from Dr. Couraud's laboratory in Paris, France [39,40]. The hCMEC/D3 cell line expressing human SSAO/VAP-1 (hCMEC/D3 hSSAO/VAP-1) was generated as described previously [41]. Considering that the proportion of vessels in brain is around 1% [42], this cell line shows SSAO/VAP-1 activity levels comparable to those observed in human brain tissue [41,26]. By contrast, non-transfected wild type (WT) hCMEC/D3 cells do not express SSAO/VAP-1, as previously demonstrated [41]. The hCMEC/D3 cells were cultured as recommended, on 150 μg/mL collagen type 1 (Rat Tail, Corning, NY, USA)-coated plates in EBM-2 (Lonza, Barcelona, Spain) medium supplemented with 5% FBS (Fetal Bovine Serum, Life Technologies, Madrid, Spain), 1.4 μM Hydrocortisone, 5 μg/mL Ascorbic Acid, 1% Chemically Defined Lipid Concentrate (Life Technologies, Madrid, Spain), 1 mM HEPES (Life Technologies, Madrid, Spain) and 1 ng/mL human bFGF (Fibroblast Growth Factor-basic), 100 U/mL penicillin and 100 μg/mL streptomycin. Cells expressing hSSAO/VAP-1 were maintained in media containing 100 μg/mL geneticin (G418, Life Technologies, Madrid, Spain) to ensure DNA maintenance. THP-1 monocytic cells were obtained from the American Type Culture Collection (ATCC, Barcelona, Spain) and grown in RPMI 1640 medium (Life Technologies) supplemented with 10% FBS. All cells were maintained at 37ºC, in a humidified atmosphere containing 5% $CO_2$.

### 2.2. BBB - Neurovascular Unit model

To mimic a NVU environment, hCMEC/D3 cells were co-cultured with mouse mixed neuron-glia primary cultures. hCMEC/D3 cells were seeded at 2 x $10^5$ cells/ml in collagen and fibronectin-coated 12-well Transwell inserts (Transwell polyester membrane inserts, pore size 0.4 μM, Corning, NY, USA) and allowed to grow for 3 days in vitro (DIV). At 3$^{th}$ DIV, hCMEC/D3 were starved in FBS, ascorbic acid and bFGF-free EBM-2 media. At 4$^{th}$ DIV, endothelial cells were put in co-culture by joining hCMEC/D3-containing inserts with 12-well plates containing 12$^{th}$ DIV neuron-glia cultures. Mouse mixed neuron-glia primary cultures were performed as described in [43], with some modifications: E14.5 – 15.5 C57BL/6 mice were used; cells were seeded on poly-D-lysine-coated plates in BME media (Invitrogen) supplemented with 5% horse serum (HS), 5% FBS, 10 mM glucose and 2 mM Glutamax; at 7 DIV, media was changed by BME supplemented with 10% HS and 10 μM cytosine arabinoside; at 12 DIV, half of the media was changed by BME with 5% HS. After 1 DIV in co-culture, endothelial cells were treated according to each type of experiment.

2.3. Cell treatments

For conditioned media treatments, media from WT and SSAO/VAP-1-expressing cells were collected after 4 days in culture under starvation conditions. This media was used to treat endothelial cells: at day 1, media from each cell type was completely changed by conditioned media from the other cell type (i.e. media from WT cells was added to hSSAO/VAP-1-expressing cells); then, half of this media was replaced by new conditioned media each 24h until day 4.

For treatment with compounds or blocking antibodies, cells were starved for 24h and then treatments were added. SSAO inhibitors semicarbazide (Sc), BTT 2079 and BTT 2089 were added 30 min before SSAO substrate (methylamine, MA) addition, and AβD ($A\beta_{1-40}$ peptide containing the Dutch mutation, Bachem AG, Hauptstrasse, Switzerland) was introduced 15 min after MA. Specific SSAO inhibitors BTT 2079 and BTT 2089 were provided by Dr. Smith (Biotie Therapies, Turku, Finland). Aβ was pretreated with 1,1,1,3,3,3-hexa-fluoro-2-propanol (HFIP), aliquoted, evaporated and stored at -80ºC until its use, being then dissolved in sterile phosphate-buffered saline (PBS) containing 0.1% ammonium hydroxide. Anti interleukin 6

blocking antibody (IL-6; MAB206-100, R&D Systems, Minneapolis, USA) or a control antibody (MAB002, R&D Systems) were added at 5 μg/μl for 48h.

2.4. Luminex assays

Media to analyze the different angioneurins of interest were obtained from inserts containing non-treated hCMEC/D3 endothelial cells expressing or not the hSSAO/VAP-1 (hSSAO/VAP-1 hCMEC/D3 vs wild type – WT cells), after 3 days of co-culture with mixed cultures. Media were kept aliquoted at -80ºC until used. Magnetic milliplex kits (Merck-Millipore, Madrid, Spain) containing detection antibodies for the following molecules were used: vascular endothelial growth factor 1 (VEGF-1); interleukins 1β, 6 and 8 (IL-1β, IL-6, IL-8); tumor necrosis factor alpha (TNF-α); fibroblast growth factor 2 (FGF-2); soluble vascular cell adhesion molecule 1 (sVCAM-1); soluble inducible cell adhesion molecule 1 (sICAM-1); nerve growth factor (NGF); E and P-selectins (E-sel, P-sel), transforming growth factor beta 1 (TGF-β1) and insulin growth factor 1 (IGF-1). Angioneurins were detected by Milliplex MAP Human Magnetic Bead Panels following the manufacturer instructions. Quantification was performed with a Magpix analytical test instrument xPONENT (Luminex, Austin, TX, USA) and xPONENT 4.2 software (Luminex), with support of the technical staff in the INc (Neurosciences Institute, UAB, Barcelona).

2.5. Western blot analysis

Equal amounts of protein (20 μg per lane), determined by the Bradford method (Bio-Rad, Barcelona, Spain) were separated by SDS-PAGE and transferred onto nitrocellulose membranes. For Aβ detection, 12% bistris/bicine polyacrylamide gels were used as previously described [44] and proteins were transferred onto polyvinylidene fluoride membranes (PVDF; GE Healthcare, Barcelona, Spain). After blocking with tris-buffered saline with 0.1% Triton X-100 (TBST) plus 5% non-fat dry milk (10% non-fat dry milk and 0.1% bovine serum albumin for Aβ gels) for 1h, they were incubated overnight at 4ºC with the corresponding primary antibody: VCAM-1 (1:000) (3540-S; Epitomics, Burlingame, CA, USA); ICAM-1 (1:1000) (GTX100-450; GeneTex, Barcelona, Spain); Zona Occludens 1 (ZO-1, 1:1000) (40-2200; Life Technologies); Glyceraldehyde 3-phosphate dehydrogenase (GAPDH, 1:20,000) (ADI-CSA-335; Enzo Life Sciences, New York, NT, USA); Claudin-5 (1:500) (sc-374221; Santa Cruz Biotechnology, Dallas, TX USA); VE-Cadherin (1:500) (sc-9989; Santa Cruz Biotechnology); Signal transducer

and activator of transcription 3 (STAT3, 1:1000) (sc-8019; Santa Cruz Biotechnology); phospho-STAT3 (p-STAT3, 1:1000) (sc-8059; Santa Cruz Biotechnology); Matrix Metalloproteinase 2 (MMP-2, 1:1000) (ab37150; Abcam, Bristol, UK); Matrix Metalloproteinase 9 (MMP-9, 1:1000) (ab7299; Abcam); Tissue Inhibitor of Metalloproteinases (TIMP-1, 1:2000) (ab38978; Abcam); Low density lipoprotein receptor-related protein 1 (LRP-1, 1:10 000) (2703-S; Epitomics); VEGF Receptor 2 (VEGFR2, 1:1000) (1672479S; Cell Signaling Technology, Danvers, MA, USA); phospho-VEGFR2 (pVEGFR2, 1:1000) (1674991T; Cell Signaling Technology); Cleaved Caspase-3 (1:1000) (9661; Cell Signaling Technology); Bax (1:1000) (2772; Cell Signaling Technology); Bcl-2 (1:1000) (610538; BD Biosciences, San Jose, CA, USA); Amyloid precursor protein (APP, 1:1000) (antibody generated by the 20.1 hybrydoma cell line, a kind gift from Dr. W.E. Van Nostrand, NY USA); SSAO (1:1000) [45]; beta actin (β-actin, 1:10000) (A1978; Sigma). Secondary HRP (horseradish peroxidase)-conjugated antibodies used were anti-mouse IgG (1:2000) (P0161; Dako, Madrid, Spain) and anti-rabbit IgG (1:2000) (554021; BD Biosciences). Blots were developed using ECL® Chemiluminiscent detection reagents and High Performance Chemiluminiscence Films (GE Healthcare). The ImageJ software (National Institutes of Health, USA) was used to quantify the western blot signals.

2.6. Immunocytofluorescence

Cells were grown on collagen-I-coated glass coverslips and fixed in methanol-acetic acid (3:1) at -20ºC for 20 min at the indicated times after reaching confluence. After permeabilization with PBS containing 0.2% Triton X-100 (PBST) for 30 min, cells were blocked with PBST containing 0.2% gelatin, 20 mM glycine and 5% FBS for 20 min. Then, cells were incubated with primary antibodies (ZO-1, 1:100, 1874-30, Life Technologies; APP, 1:500) in blocking solution with 3% FBS overnight at 4ºC with the addition of 30 min at room temperature. After washing with PBS, secondary antibody (Alexa Fluor 568 goat anti-rabbit IgG, 1:1000, Life Technologies) was added in the same buffer as the primary antibody for 1 h at room temperature, and cell nuclei were contrasted with Hoechst 33258 (1:1000). Coverslips were mounted on slides with Mowiol mounting media. Images were taken using the Zeiss LSM700 confocal microscope at the microscopy facility of the INc in UAB.

2.7. Cell viability

For the determination of cell viability by 3-(4,5-dimethylthiazol-2-yl)2,5-diphenyl-tetrazolium bromide (MTT) reduction assay, MTT solution (0.5 mg/mL, final concentration) was added to the cells 1 h before the end of treatments. The medium was then replaced by dimethyl sulfoxide to dissolve the formazan blue precipitate formed, which was quantified at 560 and 620 nm in a microplate reader (Synergy HT and data analysis software KC4, Bio-Tek Instruments Inc, Winooski, VT, USA).

For the Lactate-deshidrogenase (LDH) activity assay, TOX-7 (Sigma-Aldrich) kit was used following manufacturer's instructions. Seventy-five μL of media from each well was used for the assay, performed in 96-well plates, and incubated for 1 h in the dark with LDH assay mixture. Then, absorbance was read at 490 nm, and it was subtracted the value of reading the plate at 690 nm.

2.8. Dextran assay for cell permeability determination

After 3 days of co-culture with mixed cultures or the corresponding treatments, 500 μL of DMEM medium (Invitrogen, Madrid, Spain) containing 2 mg/mL 70 kDa Fluorescein isothiocyanate-dextran were added replacing the insert culture media. The permeable filter inserts were then changed to 12-well plates containing pre-warmed DMEM and sequentially transported to new wells at 5 min intervals for 30 min. Cells were maintained at 37ºC during the process. At the end, the fluorescence of each well (lower chamber of the inserts) was measured (485 nm and 520 nm ex/em) and apparent permeability coefficients (Pe; cm/sec) were calculated from curves slopes (fitted using linear regression) obtained by plotting cumulative volume cleared against time, for all experimental conditions. Non-treated cells (NT), or WT cells for comparing basal conditions were used as controls, and differences in permeability coefficients were expressed as % of control.

2.9. Transendothelial electrical resistance

Transendothelial electrical resistance (TEER) of endothelial cells seeded on inserts was measured at 0, 6, 24, 48 and 72h after the co-culture establishment with mixed cultures. TEER measurements were recorded using a STX2 probe with EVOM2 (World Precision Instruments, Sarasota, USA). In each experiment, the average of three different readings was used for each insert.

2.10. Adhesion assays

For adhesion assays, hCMEC/D3 cells were seeded on 24-well plates. THP-1 monocytes were labeled with 1 μM Calcein-AM for 30 min, and then added to endothelial cells (2.5 x 105 THP-1 cells per well). After 30 min incubation at 37ºC, unbound monocytes were removed by turning over the plates onto absorbent paper, carefully adding FBS-free RPMI 1640 medium to the plates with an auto-pipette, and repeating the washing for three times. The fluorescence intensity was measured using a microplate reader ($\lambda_{ex}/\lambda_{em}$: 495/530 nm) (Synergy HT and data analysis software KC4; Bio-Tek Instruments Inc.). Micrographs were taken using a Nikon Eclipse TE 2000-E inverted fluorescence microscope and a Hamamatsu C-4742-80-12AG camera and Metamorph® Imaging System software.

2.11. MMPs activity

For the measurement of MMP-2 and MMP-9 activity, it was used the fluorimetric assay SensoLyte ® 520 MMP-2 Assay Kit (Anaspec, AS-71151), according to the manufacturer's instructions. Briefly, cells were lysed in the recommended buffer and kept at -80ºC until their use. First, dose and time curves were performed to determine the best conditions for the incubation with the substrate. Then, equal amounts of protein were incubated at 37ºC for 90 min and the cleavage of a FRET peptide that releases the fluorescent 5-FAM from its quencher QXL520 was measured at ex/em 490/520 nm with the fluorescence microplate reader. The concentration of this substrate for each sample was obtained by interpolation into a reference standard concentration curve. Data were normalized for each experiment to the values obtained in the WT cells and presented as percentage of change in MMPs activity versus WT cells.

2.12. Statistical analysis

Results are given as mean ± SEM of independent experiments. Statistical analyses were performed by one-way ANOVA tests followed by a Newman-Keuls or Bonferroni multiple comparison tests when comparing more than 2 conditions; statistical differences between 2 conditions were evaluated by unpaired Student's *t*-test. A two-way ANOVA test was performed when the influence of 2 independent variables on one independent variable were analyzed. A $p < 0.05$ was considered to be statistically significant, according to the following significance

levels: ***$p < 0.001$, **$p < 0.01$ and *$p < 0.05$. Statistical analyses and graphic representations were obtained with Graph-Pad Prism 6.0 software (San Diego, CA, USA).

## 3. Results

### 3.1. The expression of SSAO/VAP-1 induces brain endothelial activation towards a pro-inflammatory phenotype.

Previous work in our laboratory showed that an increase in SSAO/VAP-1 was related to endothelial dysfunction and AD [46,36]. In one hand human umbilical vein endothelial cells (HUVECs) expressing SSAO/VAP-1 showed enhanced cell toxicity in the presence of Aβ *in vitro* [36], while on the other hand, we observed increased SSAO/VAP-1 in brain vessels from AD patients [46]. Thus, in the present work we decided to study whether the expression of SSAO/VAP-1 in human brain endothelial cells was able to alter the release of a group of angioneurins that have been associated to AD or to endothelial dysfunction throughout bibliography (Table 1). Their basal release was quantified in culture media obtained from human cerebral microvascular endothelial cells expressing or not the hSSAO/VAP-1 [41], after being co-cultured with neuron-glia mixed cultures to generate a NVU environment (Fig. 1).

| | EXPRESSION | | Functions in AD | | Described in | References |
|---|---|---|---|---|---|---|
| | ECs | N+G | ECs | N+G | AD patients | |
| **VEGF** (Vascular endothelial growth factor) | +++ | + | Angiogenesis, vascular permeability and dilation, cell migration, proliferation, differentiation and survival | Neurogenesis, neuronal and glial survival, neuronal proliferation, neuronal and glial migration, axon growth and dendritic arborization | Increased in CSF | 1, 14, 47, 48 |
| **TGF- β** (Transforming growth factor) | + | +++ | Angiogenesis, VEGF induction and maintenance of the BBB integrity | Neuroprotection, glial scar and microglia activation | Increased in plasma and CSF. Decreased in serum | 1, 14, 47, 49, 50 |
| **NGF/pro-NGF** (Nerve growth factor) | + | +++ | Angiogenesis, cell survival, proliferation, migration and VEGF induction | Neuroprotection, neuronal survival | Increased in serum and CSF | 14, 47 |
| **FGF-2** (Fibroblast growth factor) | + | + | Angiogenesis, cell proliferation, VEGF induction and maintenance of the BBB integrity | Neuroprotection, neuronal survival, synaptic stimulation and glial differentiation | Not changed | 14, 47 |
| **IGF-1** (Insulin like growth factor) | + | + | Angiogenesis, survival, migration, proliferation and inflammatory responses | Neuronal/glial growth and survival, neuronal differentiation, migration, cytoskeletal assembly, synaptic formations and myelinic production/maintenance | Increased in plasma | 14, 47, 51, 52 |
| **TNF- α** (Tumor Necrosis Factor) | + | +++ | Blood vessels remodeling, adhesion molecules and cytokines induction | Neurotoxicity, dysregulation of synaptic transmission, inhibition of synaptic plasticity, and microglia activation | Increased in plasma/serum and CSF | 1, 14, 47, 50, 53 |
| **IL-6** (Interleukin 6) | + | + | Angiogenesis, adhesion molecules upregulation | Neurogenesis, neuroprotection, gliogenesis, neuronal and glial differentiation and proliferation. | Increased in plasma/serum and CSF | 1, 47, 50, 53 |
| **IL-8** (Interleukin 8) | + | + | Unknown | Unknown | Increased in plasma/serum | 1, 53, 54 |
| **IL-1β** (Interleukin 1β) | + | +++ | IL-6 and TNF-α induction, early initiation of the inflammatory response, adhesion molecules upregulation | IL-6 and TNF-α induction, neuroinflammation, neurotoxicity, microglia and astrocyte activation and differentiation | Increased in plasma/serum | 1, 47, 50, 53, 55 |
| **ICAM-1**/CD54 (intercellular adhesion molecule) | + | - * | Angiogenesis, proinflammatory cytokines induction, transendothelial migration of leukocytes | Proinflammatory cytokines induction | Increased in plasma/serum | 47, 56, 57, 58 |
| **VCAM-1**/CD106 (vascular cell adhesion molecule) | + | - * | Inhibition of cell extravasation, alteration of TJs morphology | Proinflammatory cytokines induction | Increased in plasma | 47, 58, 59, 60 |
| **ELAM-1**/CD62E or E-selectin (endothelial leucocyte adhesion molecule) | + | - | Chronic inflammation | Unknown | Not changed | 47, 58, 61 |
| **LRP-1** (low density lipoprotein receptor-related protein 1) | ++ | ++ | Efflux of brain Ab, opening of BBB, MMPs induction | Cell signaling, calcium entrance regulation, Ab production and clearance | Decreased (controversy) | 62, 63, 64, 65, 66, 67, 68 |
| **RAGE** (receptor for advanced glycation endproducts) | ++ | + | Influx of Ab into brain, oxidative stress, increase of proinflammatory cytokines | Oxidative stress and inflammation, Ab production increase, neurotoxicity and synaptic loss | Increased in brain tissue | 69, 70, 71, 72 |

**Table 1. Angioneurins released by endothelial cells, neurons and glia, selected as candidates tested in our study due to their potential involvement in AD.** All cell types (endothelial cells, ECs; neurons and glia, N+G) express receptors for all the angioneurins listed in the table. "+++" means that the molecule is mostly expressed by this cell/s type/s over the other/s, while "+" means that is expressed at lower levels and "-" means that no expression has been found. * Some authors found VCAM-1 and ICAM-1 expression in neurons [73], but there is no recent data about it.

Results showed that the release of trophic factors VEGF, TGFβ-1 and NGF is significantly higher in endothelial cells expressing hSSAO/VAP-1, while they display a non-significant reduced trend to release FGF-2 compared to WT cells, that do not express the protein (Fig. 1A). No changes were detected in IGF-1, whose levels were similar to those measured in cell culture media (Fig. 1A and Suppl Fig. 1). On the other hand, regarding the release of molecules related with inflammatory processes, it was observed that cells expressing hSSAO/VAP-1 release significantly higher amounts of IL-6 and IL-8 (Fig. 1B). IL-1β and TNF-α were also analyzed but they were not detected. Moreover, hSSAO/VAP-1-expressing cells release significantly higher levels of the soluble form of the adhesion protein VCAM1 (sVCAM-1) (Fig. 1C). A trend in the same line was observed in case of soluble ICAM-1 (sICAM-1), and E and P-selectins were not detected. The membrane-bound forms of both VCAM-1 and ICAM-1 are significantly increased in cells expressing hSSAO/VAP-1 as well (Fig. 1D). Similar results were obtained in angioneurins released from endothelial cells without being co-cultured with neuron-glia mixed cultures (data not shown) suggesting that changes in angioneurins release induced by SSAO/VAP-1 expression is cell autonomous, and not influenced by the neurovascular context. Treatments with MA and/or AβD did not induce significant changes compared to the basal levels in each cell type (Suppl Fig. 1).

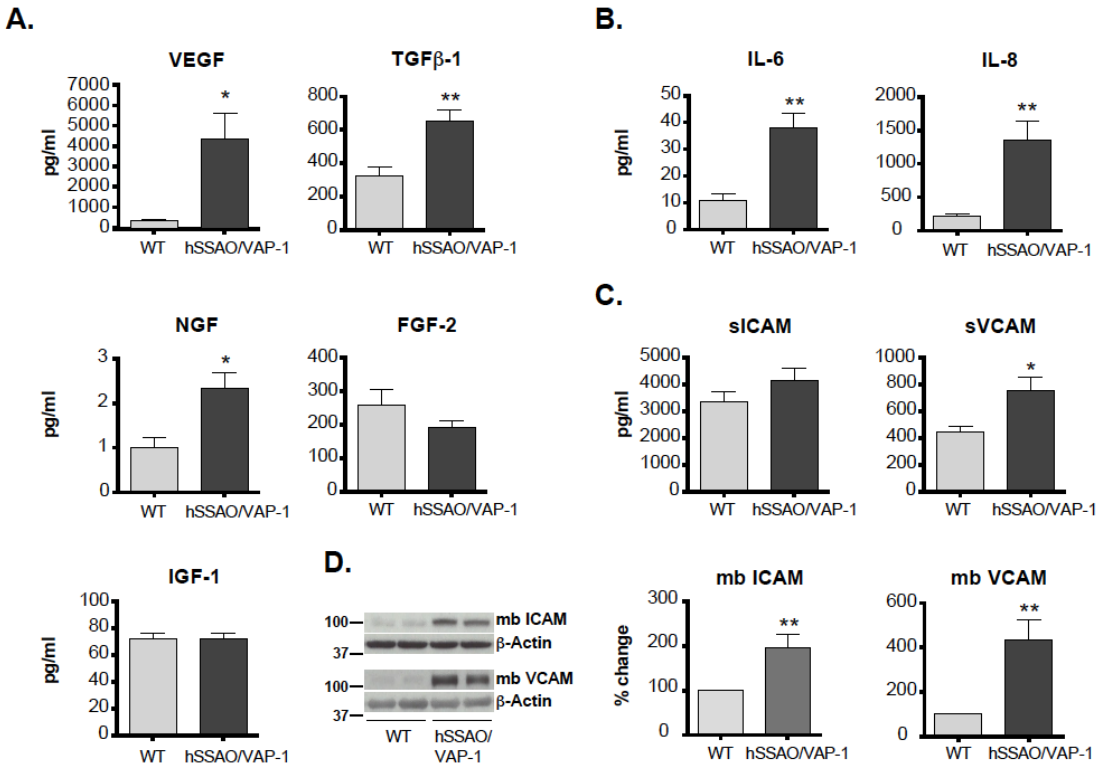


**Figure 1. The secretion of angioneurins is altered in hSSAO/VAP-1-expressing hCMEC/D3 cells.** (A) Levels of trophic factors VEGF, TGFβ-1, NGF, FGF-2 and IGF-1, (B) pro-inflammatory interleukins IL-6 and IL-8, and (C) soluble vascular adhesion proteins sICAM and sVCAM quantified by Luminex in the media of WT and hSSAO/VAP-1-expressing hCMEC/D3 cells co-cultured for 3 days with mouse brain mixed primary cultures. (D) Membrane-bound forms of VCAM-1 and ICAM-1 determined by western blot in cell lysates after 3 days in confluence. Beta actin was used as loading control. Data is expressed as mean ± SEM of quantifications (pg/ml) in A-C, or of percentage change vs WT in D, obtained from at least 4 independent experiments. *p<0.05, **p<0.01.

### 3.2. Human brain endothelial cells expressing hSSAO/VAP-1 show increased basal blood-brain barrier permeability.

An endothelial pro-inflammatory phenotype may be associated to the alteration of the BBB permeability in order to allow the pass of peripheral inflammatory cells through the barrier [74]. As our cells showed an increased release of pro-inflammatory angioneurins, when BBB function of endothelial cells expressing hSSAO/VAP-1 was studied, it was observed that they show an increased basal permeability to 70 KDa Dextran (Fig. 2A), as well as decreased TEER ($\Omega/cm^2$) throughout time (Fig. 2B). A two-way ANOVA of time and genotype (WT or hSSAO/VAP-1) on TEER revealed significant main effect of time [$F(4, 20) = 2.936$, $p<0.05$*] and genotype [F (1,

20) = 10.96, p<0.01**], with non-significant time x genotype interaction [F (4, 20) = 1.268, p=0.32]. In addition, hSSAO/VAP-1-expressing endothelial cells display an increased ability to bind leukocytes compared to WT cells, as indicated by a significantly higher THP-1 adhesion in basal conditions (Fig. 2C). These functional alterations may be related to the decreased expression of the tight junction-related proteins ZO-1 and claudin-5 (Fig. 2D), and the adherens junction-related protein VE-cadherin (Fig. 2E) in endothelial cells expressing hSSAO/VAP-1. In the same line, immunofluorescence images obtained by confocal microscopy of ZO-1 (red) revealed a ZO-1 location compatible with that of tight junctions only in WT cells, while it was completely delocalized in hSSAO/VAP-1-expressing cells, analyzed at different time points (Fig. 2F). Matrix MMP-2 and MMP-9, proteins involved in extracellular matrix stability and degradation in inflammatory conditions, were also evaluated. MMP-2 protein was increased in hSSAO/VAP-1 cells, while MMP-9 was not changed between both cell types (Suppl Fig. 2A). However, the overall gelatinase activity levels were higher in WT cells (Suppl Fig. 2B), which could be explained by an increase of the endogenous MMP inhibitor TIMP-1 in hSSAO/VAP-1-expressing cells (Suppl Fig. 2C).

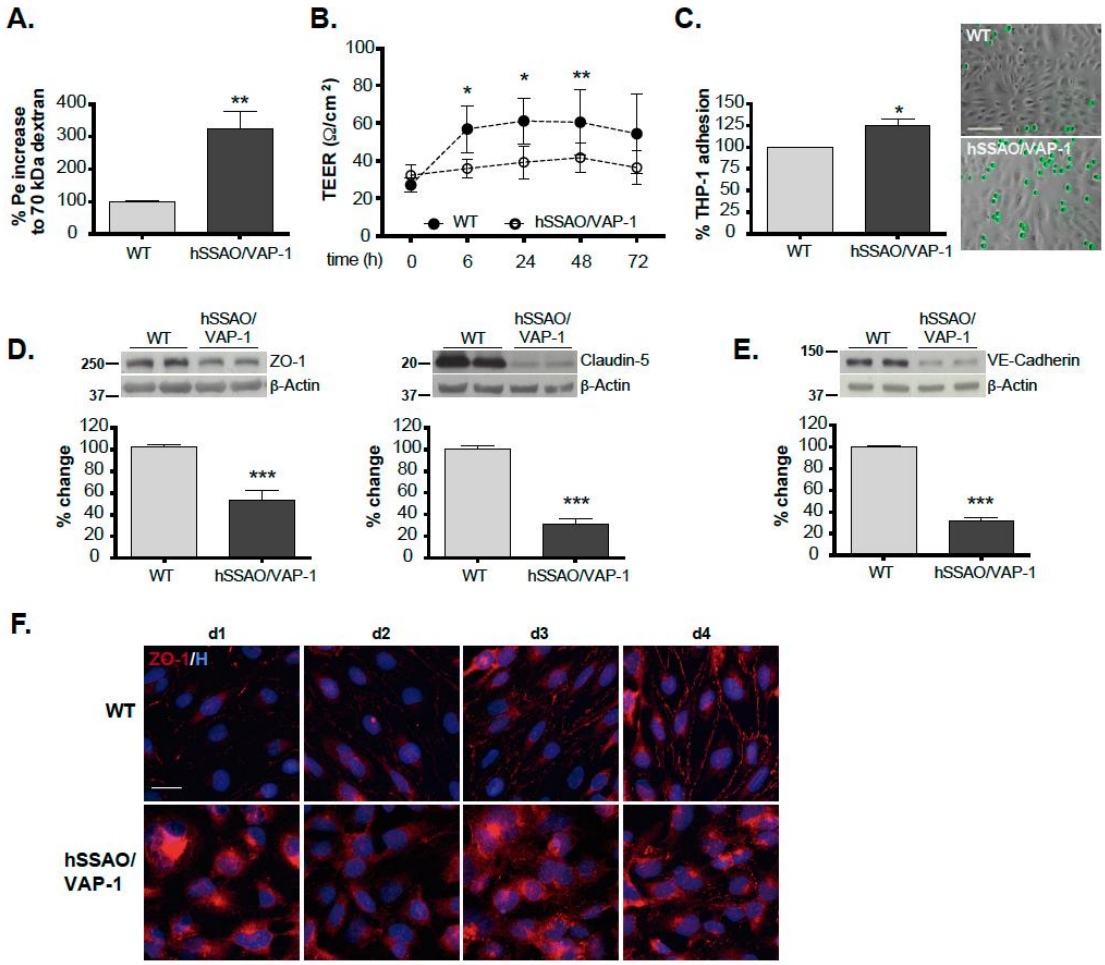


**Figure 2. hSSAO/VAP-1-expressing hCMEC/D3 cells display an increased basal BBB permeability and leukocyte adhesion.** (A) BBB functionality analyzed by transcellular permeability assay measuring the crossing of 70kDa FITC-Dextran through transwell-seeded endothelial cell monolayers co-cultured for 3 days with mouse brain primary cultures, and (B) TEER measured by an EVOM2 epithelial voltohmmeter in the same cells at different times (0, 6, 24, 48 and 72h) from the co-culture beginning. Data are expressed as mean ± SEM of percentage in permeability increase and $\Omega/cm^2$, respectively, from at least 3 independent experiments. (C) Basal endothelial inflammatory function by leukocyte-adhesion assay using Calcein-AM-labelled THP1 leukocytes in WT and hSSAO/VAP-1-expressing cells. Representative images show THP1 leukocytes (green) adhesion on endothelial cell monolayers. Scale bar: 100 μM. (D) BBB structure of hCMEC/D3 cells after 3 days confluence in culture, studied by western blot determination of the tight junctions-related proteins ZO-1 and claudin 5, and (E) the adherens junctions-related protein VE-cadherin levels. Results are expressed as mean ± SEM of at least 3 independent experiments. Beta-actin was used as loading control. Representative images are shown for each graph. (F) ZO-1 cell distribution determined by immunofluorescence and confocal microscopy at days 1, 2, 3 and 4 post-confluence; ZO-1, red; Hoechst (H), blue. Scale bar: 20 μM. *p<0.05, **p<0.01 and ***p<0.001. In B, * indicates differences vs time 0.

### 3.3. The angioneurins secreted by hSSAO/VAP-1-expressing human brain endothelial cells are able to activate their own signaling pathways and contribute to disturbing BBB functions.

Next, we aimed to determine whether the higher levels of the angioneurins released by hSSAO/VAP-1-expressing cells are able to induce changes in endothelial cell signaling, and therefore could be responsible of the functional alterations found in these cells. To this end, we analyzed the basal activation status of the molecular pathways activated by VEGF, IL-8 and IL-6 related to BBB permeability, as they showed the greatest increases in hSSAO/VAP-1-expressing cells (see Fig. 1). Because it has been reported that IL-8-induced endothelial permeability requires the transactivation of VEGFR-2 through the IL-8 receptor CXCL8 activation [54], both VEGF and IL-8 action on BBB were studied by determining the VEGFR2 phosphorylation levels at tyrosine 951, a major autophosphorylation site located in the kinase insert domain, indicator of receptor activation [75] and related with vascular permeability [76]. Results revealed almost no VEGFR2 phosphorylation in WT endothelial cells (Fig. 3A). Surprisingly, VEGFR2 expression was drastically reduced in hSSAO/VAP-1-expressing cells. On the other hand, IL-6 action was evidenced by the activation of the STAT3 pathway, since increased levels of pSTAT3 were observed in hSSAO/VAP-1-expressing cells compared to WT cells (Fig. 3B).

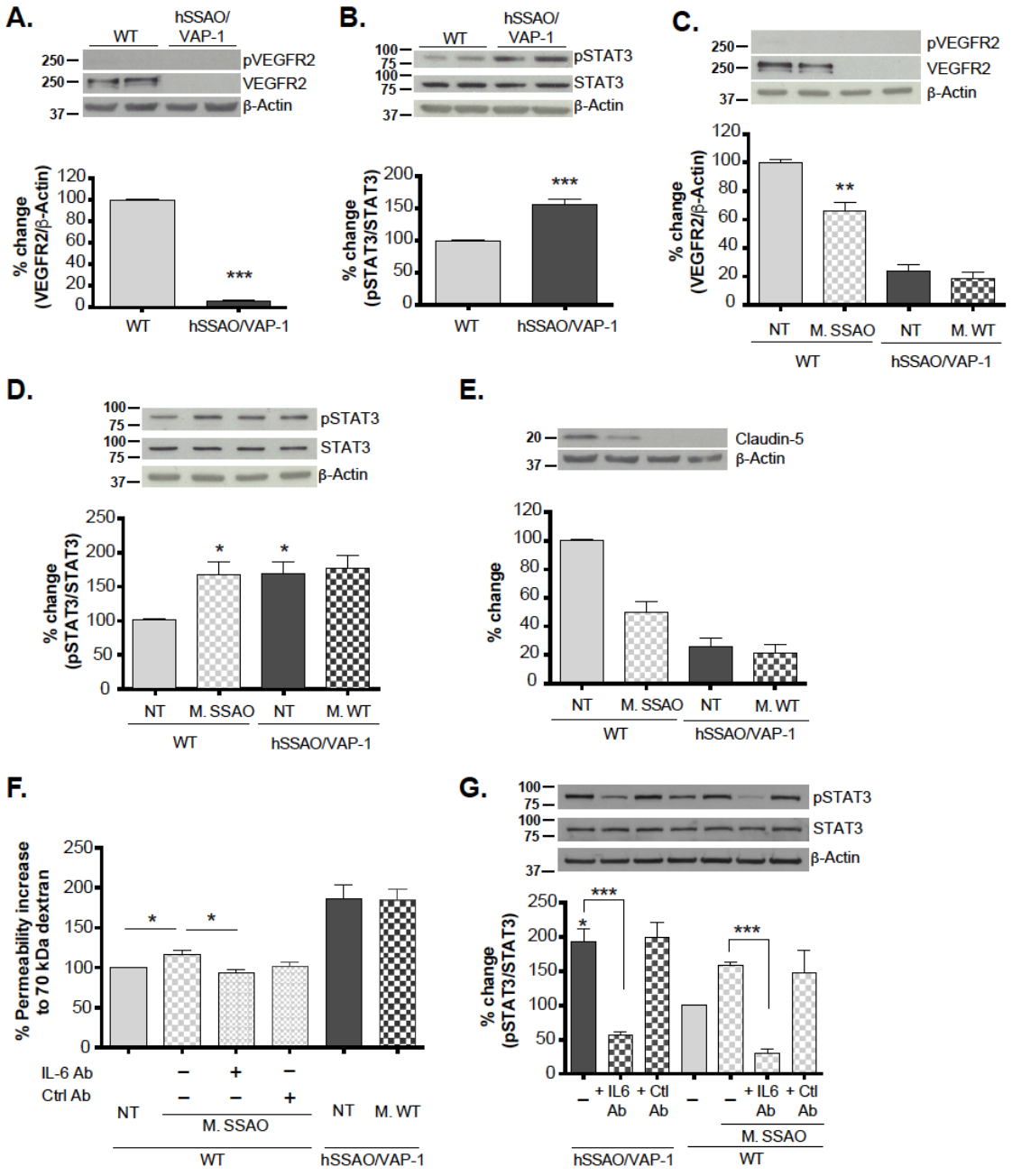


**Figure 3. Secreted angioneurins alter VEGF and IL-6 signaling pathways and contribute to the BBB leakage.** (A) Basal activation status of IL-8/VEGF and (B) IL-6 molecular pathways through pVEGFR2/VEGFR2 and pSTAT3/STAT3 determination by western blot. For VEGFR2, only the total form was quantified and represented in the graphs, as its phosphorylation form was almost non-detected. Beta actin and the total form of STAT3 were used as loading controls. (C) Effect of 4 days-conditioned media from WT and hSSAO/VAP-1-expressing cells on VEGFR2 and (D) STAT3 activation in hSSAO/VAP-1 and WT cells, respectively, analyzed by western blot. Initial media was changed by conditioned media at day 1, and half of this media was replaced by new conditioned media each 24h until day 4. (E) Effects of conditioned media on the tight junction protein claudin-5, analyzed by western blot. (F) Permeability to 70kDa FITC-Dextran of the endothelial cell monolayers in presence of conditioned media and IL-6 blocking or control antibodies (added at 5 μg/ml). (G) Effect of IL-6 blocking antibody or a control antibody on the phosphorylation status of STAT3. Data in graphs is represented as

mean ± SEM of percentage change from at least 3 independent experiments. *p<0.05, **p<0.01 and ***p<0.001 vs WT NT or as indicated.

To confirm the involvement of these over-released angioneurins in the activation of these molecular pathways, it was collected conditioned media from WT and hSSAO/VAP-1-expressing endothelial cells after 4 days in culture. Then, WT cells were treated for 4 days in the presence of hSSAO/VAP-1 conditioned media, and hSSAO/VAP-1-expressing cells were cultured in WT-conditioned media. During the treatments, half of the media was replaced by new conditioned media every 24 h to maintain the levels of angioneurins similar to those of the conditioned medias. Results showed that media from hSSAO/VAP-1 cells induces a decrease in VEGFR2 expression (Fig. 3C) and an increase in pSTAT3 levels in WT cells (Fig. 3D). However, media from WT cells is not able to restore VEGFR2 expression or to decrease STAT3 activation levels.

Then, to explore whether the differential release of angioneurins observed in both cells is the responsible of the BBB disturbances detected in hSSAO/VAP-1-expressing cells, tight junction proteins were determined by western blot after treatments with conditioned media (Fig. 3E). In line with that previously observed, WT cells treated with hSSAO/VAP-1-conditioned media showed a decreased amount of claudin-5, while WT-conditioned media in hSSAO/VAP-1-expressing cells did not modify its expression. Surprisingly, neither ZO-1, nor VE-cadherin amounts were modified in WT or in hSSAO/VAP-1-expressing cells by conditioned media treatments (Suppl Fig. 3). Permeability to 70-KDa dextran was also determined in cells after treatment with conditioned media as a BBB functional parameter (Fig. 3F). Results showed a small increase in Pe in WT cells treated with hSSAO/VAP-1-conditioned media, but not reaching the high Pe values observed in hSSAO/VAP-1-expressing cells in basal conditions. In addition, IL-6 blocking antibody prevented this Pe increase induced by hSSAO/VAP-1 conditioned media on WT cells. Again, no changes were observed in hSSAO/VAP-1-expressing cells in the presence of WT-conditioned media. To confirm the STAT3 pathway modulation by conditioned media from hSSAO/VAP-1 cells, STAT3 phosphorylation was evaluated by western blot after conditioned media and IL-6 blocking antibody treatments (Fig. 3G). Results confirmed the increase of pSTAT3 in WT cells treated with hSSAO/VAP-1-conditioned media, and its

prevention by the blocking of IL-6 as well as the decrease of pSTAT3 in hSSAO/VAP-1 cells treated with the IL-6 blocking antibody. The control antibody did not induce any change in Pe or STAT3 phosphorylation.

**3.4. Endothelial cells expressing hSSAO/VAP-1 show a positive feedback loop with AβD, enhancing its vascular deposition and inducing BBB function alterations and cytotoxicity.**

Alterations observed in BBB between WT and hSSAO/VAP-1-expressing cells were only partially explained by the differential release of proteins from both endothelial cells. Thus, we then explored other possible alterations in BBB affected by the presence of SSAO/VAP-1, focused on the AD context. Mainly $A\beta_{40}$ is deposited on cerebral blood vessels inducing Cerebral Amyloid Angiopathy (CAA), although $A\beta_{42}$ can be also deposited in small capillaries [77,78]. Endothelial cells were therefore first treated with $A\beta_{40}$ containing the Dutch mutation (AβD), a vasculotropic form of Aβ, and its deposition on endothelial cells was measured. It was observed by western blot that higher amounts of AβD were deposited on endothelial cells expressing hSSAO/VAP-1 (Fig. 4A). To explore whether this AβD deposition was dependent on SSAO/VAP-1 enzymatic activity, the same experiment was performed adding MA as SSAO substrate, and BTT 2079 as SSAO specific inhibitor. Results showed that, besides the higher deposition on cells expressing hSSAO/VAP-1, AβD deposition was also enhanced in the presence of MA only in hSSAO/VAP-1-expressing cells (Fig. 4B). The addition of the SSAO inhibitor BTT 2079 restored AβD deposition levels to the basal ones in these cells, while neither MA, nor inhibitor addition modified AβD deposition on WT cells. This effect was confirmed by immunofluorescence analysis (Fig. 4C). Same experiments were performed using $A\beta_{42}$, but no significant differences in $A\beta_{42}$ deposition were found between WT and hSSAO/VAP-1-expressing cells and only a trend was observed among different treatments (Suppl Fig. 4A). To explore possible differences in other proteins involved in Aβ processing or transport, the basal levels of APP, receptor for advanced glycation end-products (RAGE) and LRP-1 were determined (Suppl Fig. 4B). While APP and RAGE were not different between WT and hSSAO/VAP-1 cells, LRP-1 was highly expressed by the latter, although treatments with MA and/or AbD did not induce significant changes of LRP-1 in any of the cell types (Suppl Fig. 4C).

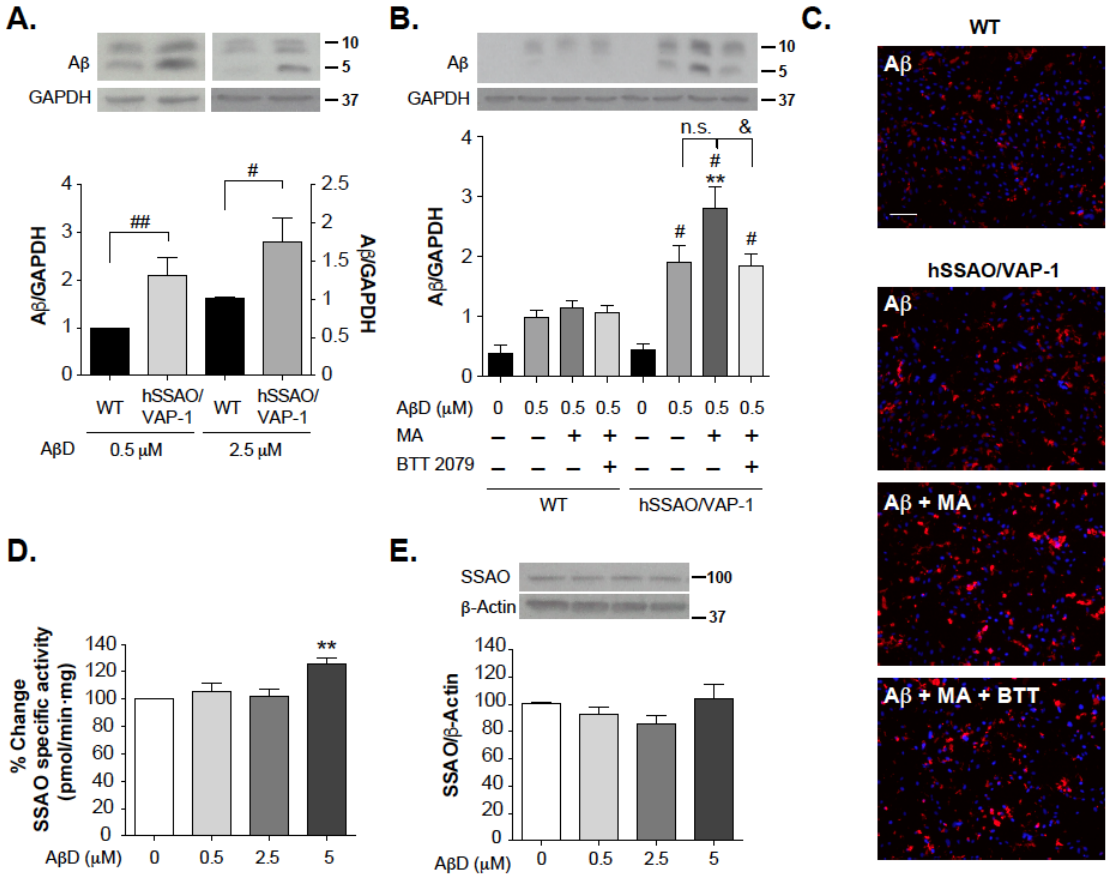


**Figure 4. Positive feedback loop between AβD aggregation and SSAO/VAP-1.** (A) Basal AβD deposition on WT and hSSAO/VAP-1-expressing hCMEC/D3 cells determined by tris/bicine western blots after 48h of AβD treatment (0.5 and 2.5 μM). (B) AβD deposition on cells after 48h treatment with AβD (0.5 μM), the SSAO substrate MA (1 mM) and its specific inhibitor BTT2079 (10 μM, added as 30 min pre-treatment), measured by western blot or (C) by Aβ immunofluorescence (red). Cell nuclei were stained with Hoechst (blue); scale bar: 100 μM. (D) SSAO specific activity and (E) protein levels were measured in hCMEC/D3 hSSAO/VAP-1-expressing cells in the presence of different concentrations (0.5, 2.5 and 5 μM) of AβD for 48h. SSAO enzymatic activity (pmol/min · mg of protein) was determined with the radiometric method using $^{14}$C-benzylamine as substrate. Protein levels were analyzed by western blot, using β-Actin or GAPDH as loading controls. Representative western blot images are shown for each quantification graph. Data in graphs is expressed as mean ± SEM of at least 3 independent experiments. **p<0.01 vs non-treated cells; $^{\#}$p<0.05 and $^{\#\#}$p<0.01 vs same treatment in WT cells; $^{\&}$p<0.05 as indicated.

On the other hand, it was also studied a possible effect of AβD presence on SSAO/VAP-1 enzymatic activity and protein levels. AβD treatment of hSSAO/VAP-1-expressing cells induced an increase in the SSAO enzymatic activity (Fig. 4D), which was not significant at the protein

levels (Fig. 4E). Similar results were observed with $A\beta_{42}$, but at lower concentrations compared to AβD (Suppl Fig. 4D-E).

Then, BBB function was first explored by Pe determination in WT and hSSAO/VAP-1-expressing endothelial cells treated with MA, AβD and BTT. Besides the basal higher Pe already observed in hSSAO/VAP-1-expressing cells compared to WT cells, AβD but not MA induced a significant Pe increase in hSSAO/VAP-1-expressing cells (Fig. 5A). The addition of the specific SSAO inhibitor BTT 2079 tended to decrease Pe, but this effect was not statistically significant. Interestingly, Pe was not modified in WT cells by any of these treatments. The leukocyte adhesion was also measured under same conditions (Fig. 5B,C). Both MA and AβD treatments induced an increase in leukocyte adhesion to hSSAO/VAP-1-expressing cells, an effect that was enhanced by the co-treatment with both compounds. The presence of each of two different SSAO specific inhibitors, BTT 2019 and BTT 2089, was able to partially reduce leukocyte adhesion. In WT cells, all treatments containing AβD increased leukocyte adhesion with no differences by the addition of MA or SSAO inhibitors.

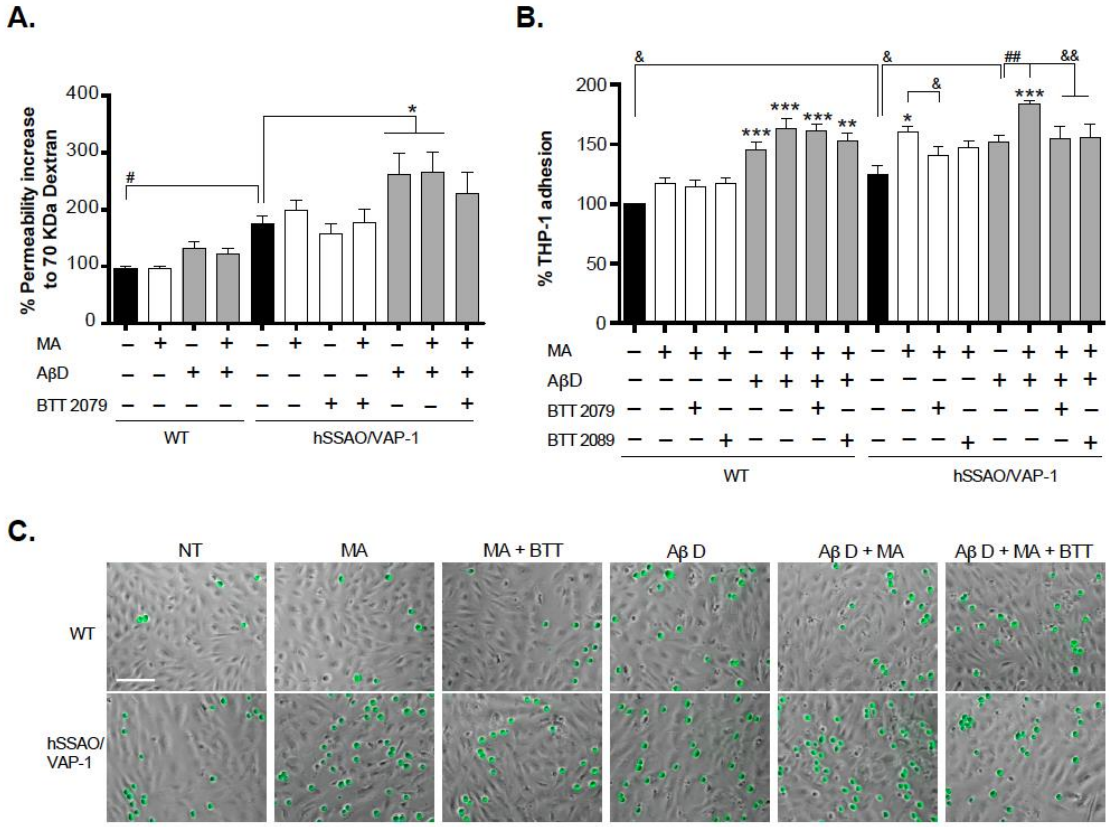

**Figure 5. The AβD-SSAO feedback induces alteration of the BBB function.** (A) Endothelial permeability to 70kDa FITC-Dextran measured in WT and hSSAO/VAP-1-expressing cells treated for 48h with AβD (5 μM), MA (1 mM) and BTT2079 (10 μM). (B,C) Endothelial leukocyte adhesion to WT and hSSAO/VAP-1-expressing cells was measured in the same conditions, adding also the inhibitor BTT2089 (1 μM). (C) Representative images showing calcein-AM-labelled THP-1 leukocytes (green) attached to endothelial cell monolayers in the same treatment conditions, using BTT2079 as inhibitor. Scale bar: 100 μM. Data in graphs are expressed as mean ± SEM of percentage difference vs non-treated cells from at least 3 independent experiments. *p<0.05, **p<0.01 and ***p<0.001 vs non-treated cells; $^{\#}$p<0.05 and $^{\#\#\#}$p<0.001 vs as indicated, by one-way ANOVA and the addition of Newman-Keuls multiple comparison test. $^{\&}$p<0.05 and $^{\&\&}$p<0.01 vs WT, NT or as indicated, by Student's *t*-test.

In addition to these functional disturbances of the BBB, the treatment of hSSAO/VAP-1-expressing cells with MA and AβD induced cytotoxicity, determined by MTT reduction (Fig. 6A), by LDH activity in media of these cells (Fig. 6B) and by the increase of the active fragment of caspase-3 (Fig. 6C) without alterations in the total caspase-3, as an indicator of apoptotic cell death induction. This cell death was not mediated by the mitochondrial cell death pathway, as indicated the absence of changes in the Bax/Bcl-2 ratio (Fig. 6D). Under these conditions, the presence of an SSAO inhibitor partly prevented the cell death induced by MA and AβD. Cytotoxicity was also evaluated treating with $A\beta_{42}$, and results showed a higher $A\beta_{42}$ cytotoxicity compared to AβD, with no additive effect due to MA treatment, and no recovery using the SSAO inhibitors in the MTT assay. However, caspase-3 activation was significantly higher in $A\beta_{42}$-MA co-treatment, and differently from AβD, the Bax/Bcl-2 ratio was significantly higher when treating with $A\beta_{42}$ and co-treating with MA. SSAO inhibitors did not induce significant recoveries when treating with $A\beta_{42}$ (Suppl. Fig. 5). The optimal treatment conditions with MA, AβD and $A\beta_{42}$ were tested previously (Suppl. Fig. 6). Thus, AβD and $A\beta_{42}$ effects were different, being the former more related to the SSAO/VAP-1 actions.

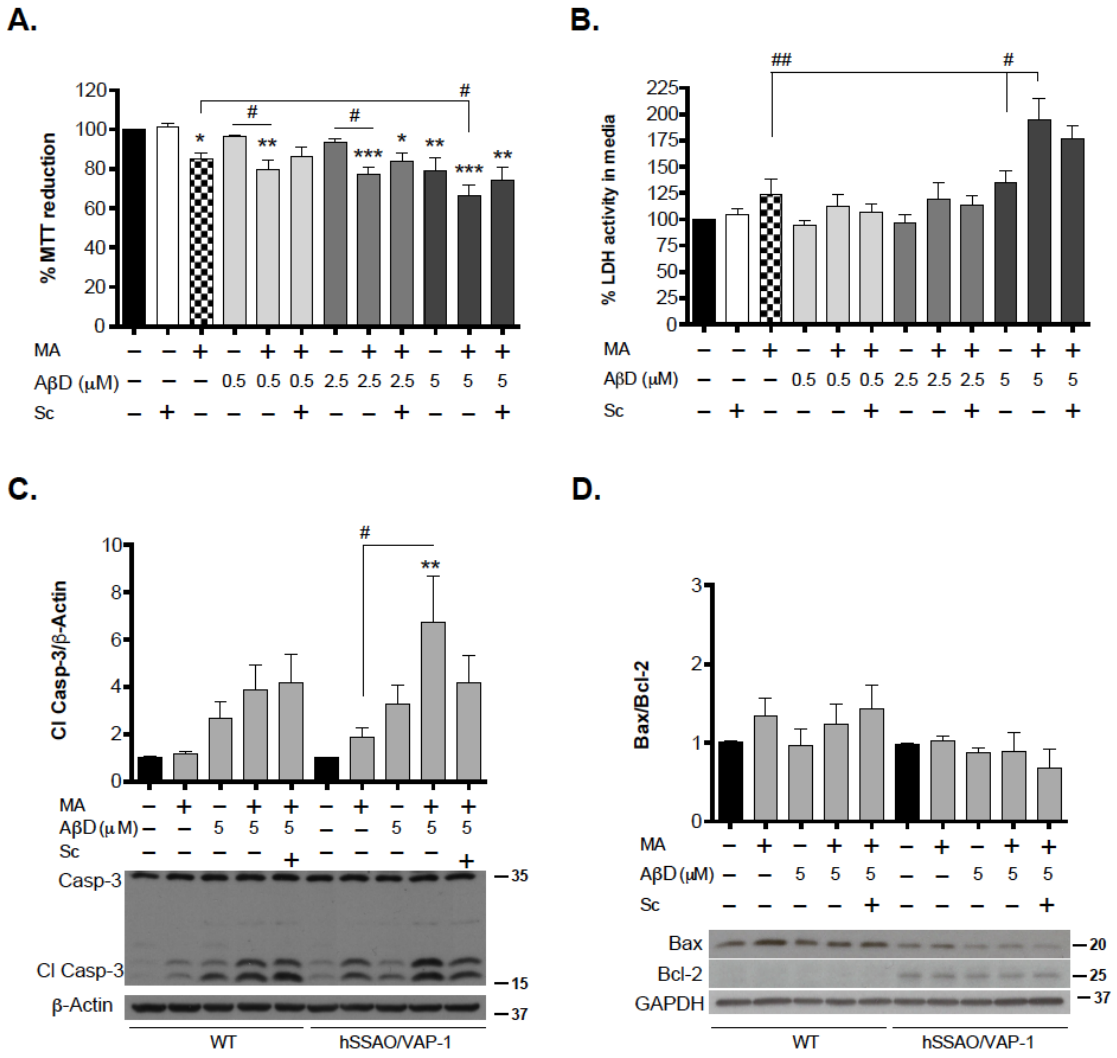


**Figure 6. The AβD-SSAO feedback induces endothelial cell toxicity.** Cell viability was determined by (A) MTT reduction or (B) LDH activity in the media in hCMEC/D3 cells expressing hSSAO/VAP-1 treated for 48h with increasing concentrations of AβD (0.5, 2.5 and 5 μM), MA (3 mM) and the SSAO inhibitor semicarbazide (Sc, 1 mM). (C) Determination of the appearance of the cleaved caspase-3 fragment (Cl Casp-3) and Bax/Bcl-2 ratio (D) in cell lysates, analyzed by western blot, under same treatments using 5 μM AβD. GAPDH was used as loading control. Representative images are shown for each protein analyzed. Data in graphs is expressed as fold change and represented by mean ± SEM values obtained from at least 3 independent experiments. *p<0.05, **p<0.01 and ***p<0.001 vs non-treated cells; #p<0.05 and ##p<0.01 as indicated, by one-way ANOVA and the addition of Newman-Keuls multiple comparison test.

## 4. Discussion

A cerebral endothelial vascular activation occurs in AD, altering the brain homeostasis and inducing the expression of interleukins (IL-1β, IL-6, IL-8), TNF-α, VEGF and MMPs, among

others [2,11,13]. SSAO/VAP-1 is also increased in plasma [24] and cerebrovascular tissue [23] of AD patients. In this regard, we have found that in our cells expressing hSSAO/VAP-1, several of these angioneurins related to inflammation (IL-6, IL-8, ICAM, VCAM) or the trophic factors VEGF, TGF-β1 and NGF were over released. VEGF regulates vessel growth in healthy and diseased tissues [79]; it is a hypoxia-inducible protein, with angiogenic behavior and vascular permeability-enhancing properties, and in AD it appears overexpressed and co-localized with Aβ plaques [80]. These data together with its increase in our vascular cells expressing hSSAO/VAP-1 corroborates the idea that cerebrovascular dysfunction plays an important role in the neurodegenerative cascade, with a possible induction through SSAO/VAP-1 actions. TGF-β1 is also increased in AD, and it is responsible of other inflammatory factors and interleukins release, contributing as well to the inflammatory process linked to this neurodegenerative disorder [81]. The TGF-β1 increase was observed in our hSSAO/VAP-1-expressing human brain endothelial cells and it was also correlated with the levels of IL-6, IL-8, VCAM and ICAM-1. NGF is a neurotrophin required to promote neuron survival pathways, and it is found normally decreased in AD [82]. Its increase in our hSSAO/VAP-1-expressing cells could be related with a compensatory signal, although other trophic factors (FGF-2, IGF-1) were not significantly modified. NGF increase could be also related with a pro-NGF increase observed in AD brains, which has been shown to induce apoptosis in neuronal cell cultures [83]. Unfortunately, our analysis method does not discriminate between NGF and pro-NGF, so we cannot confirm this possibility. In the same line, NGF is able to modify the lipid composition of neuronal membranes, therefore potentiating Aβ accumulation and cytotoxicity on these cells [84]. Whether this effect also occurs in our vascular cells, or if it could be involved in the crosstalk between Aβ aggregation and SSAO/VAP-1 effects needs to be addressed in the future, as well as the significance of this change for the neurovascular unit function.

The alterations of the angioneurins release or the reduced levels of BBB-related proteins observed in brain endothelial hSSAO/VAP-1-expressing cells, suggests that this multifunctional enzyme could be involved in protein expression regulation. Although we have not identified the molecular inductor of the structural and functional changes observed in these cells, it has been described that the products resulting from SSAO/VAP-1 enzymatic activity are able to induce E and P-selectins expression and release in HUVEC cells [33], an effect that we have not

observed in our brain endothelial cells. However, it cannot be ruled out that, since SSAO/VAP-1 is also a pro-inflammatory protein, its expression could be related to structural changes in endothelial cells that in turn, would promote a differential protein expression pattern leading to endothelial activation. Alternatively, the enzymatic metabolism of other unknown substrates could modify the protein expression, and explain the differences observed in hSSAO/VAP-1-expressing cells, such as a higher expression of VCAM-1, ICAM-1, and LRP-1 or a reduced expression of the junctional proteins VE-cadherin, claudin-5 and ZO-1. The molecular inductor of these differences, or if it is directly SSAO/VAP-1, needs further studies. On the other hand, although increased MMPs have been found in AD associated to the BBB leakage [85], the MMP-2 protein increase observed in hSSAO/VAP-1 cells seems not to be relevant for the changes observed in these cells, because the overall MMP activity was found to be lower in them. Other MMPs not analyzed in this work could be altered in hSSAO/VAP-1-expressing cells explaining this result, as the substrate used here for measuring MMPs activity can be metabolized by other MMPs besides MMP-2. In addition, the lower MMPs activity found could be related with the MMPs/TIMPs ratio, as TIMP-1 was found significantly increased in hSSAO/VAP-1-expressing cells. Interestingly, this MMPs inhibitor increase has been recently identified as a possible blood biomarker for AD [86]. Whether these changes are relevant for the endothelial activation and BBB opening phenotype observed in hSSAO/VAP-1-expressing cells, or if they are related with hSSAO/VAP-1 protein expression remains to be elucidated. In particular, MMP-2 observed changes could be related with the increase in SSAO/VAP-1 expression, as MMP-2 has been related with the SSAO/VAP-1 shedding [87].

Analyzing the functionality of brain endothelial cells expressing hSSAO/VAP-1, the observed pro-inflammatory phenotype of these cells correlated with a slight increase in basal leukocyte adhesion and with a higher permeability of the BBB formed by these cells. A dysfunctional BBB is found in AD, and it has been associated to a deficient clearance of Aβ [88] and to the contribution to an early cognitive impairment [74]. BBB tightness is controlled by transmembrane tight junction proteins that seal the paracellular gap (Claudins and Cadherins) and fix the transmembrane proteins to the actin cytoskeleton (ZO-1) [89,90]. The lack of TEER increase and ZO-1 positioning at tight junctions along different time points suggests that hSSAO/VAP-1 expressing endothelial cells are not able to close the BBB and therefore form a

functional BBB. These functional BBB disturbances may be probably explained by the decrease in the expression of claudin-5, VE-cadherin and ZO-1 in hSSAO/VAP-1-expressing cells. All these effects make sense because as an adhesion protein, SSAO/VAP-1 will promote leukocyte binding and transmigration through the endothelium, by which the BBB will need to be opened, mediated by these changes.

When evaluating the role of the over released angioneurins in these functional BBB alterations, we found that these alterations could not be explained only by the differential release of proteins between both cell types, because the secreted media did not mimic all the changes previously found in cells expressing hSSAO/VAP-1. With the conditioned media treatments, we observed the decrease in claudin-5 but not changes in VE-cadherin or ZO-1, indicating differences in the stimulus regulating these proteins. Consequently, only a slight increase in permeability was observed after treatment with conditioned media, much less evident than that of endothelial cells expressing hSSAO/VAP-1. We first attributed these changes to the most altered angioneurins, VEGF, IL-8 and IL-6, and thus we checked that their signaling pathways were consequently altered in hSSAO/VAP-1-expressing cells. VEGF and IL-8 signaling would converge in activating VEGFR2 molecular pathway in order to promote an endothelial permeability increase, as described by others [54]. However, in our cells we found a drastic reduction in the expression of VEGFR2. These results correlate with the findings that VEGF levels were found increased in plasma from AD patients, while plasma and mRNA levels of its receptors VEGFR1 and VEGFR2 were decreased in these patients [91]. Several harmful stimuli have been shown to reduce VEGFR2 expression, as oxidized low-density lipoproteins or methylglyoxal [92-94]. Interestingly, methylglyoxal is one of the metabolic products of the enzymatic activity of SSAO/VAP-1, when metabolizing aminoacetone. Although we have not observed significant differences in the release of angioneurins when treating with methylamine as SSAO substrate, we cannot rule out that other endogenous substrates could contribute to these alterations. IL-6 was the other signaling pathway analyzed as possible responsible of these BBB alterations, and in this regard, the STAT3 pathway was consequently more activated in endothelial cells expressing SSAO/VAP-1. The dependence of these changes on IL-6-activated STAT3 pathway was confirmed through the addition of an IL-6 blocking antibody, which abolished the permeability changes induced by hSSAO/VAP-1 conditioned media on WT

cells. IL-6 is a major inflammatory interleukin, and its increase has been found in AD, together with other cytokines [95], but although it is associated to dementia, it is not specific for AD, albeit it clearly affects BBB function [96].

Although we cannot rule out the participation of other soluble molecules not analyzed in this work, the results obtained with conditioned media experiments indicate that the dysfunctional alterations found in these cells cannot be completely explained by differential secretion patterns. In addition, the results also indicate that the differential secreted proteins can affect the surrounding microenvironment, and suggest that SSAO/VAP-1 expression could alter the neurovascular unit function through these released factors. For instance, it has been described that VEGF can directly affect the glutamatergic synaptic function, and the silencing of VEGFR in neural cells impairs synaptic plasticity [97]. Whether this endothelial-secreted molecules are able to reach the parenchyma and if they can mediate these or other effects under AD conditions in neural cells is currently being studied in our model.

Despite it has been described that SSAO/VAP-1 is overexpressed in CAA-AD patients, colocalizing with Aβ deposits [23,98], the exact contribution of this enzyme to this pathology and the mechanisms involved are not completely understood. The association of a BBB dysfunction, which according to our results could be promoted by SSAO/VAP-1 expression, with the impairment of Aβ clearance, prompted us to study the relationship between SSAO/VAP-1 and Aβ in these brain microvascular endothelial cells. By treating cells with the vasculotropic AβD, we observed that AβD was highly deposited on hSSAO/VAP-1-expressing. This effect observed was both dependent and independent of the SSAO enzymatic activity using MA as substrate. Similar results were previously observed in HUVEC cells [36], and on the other hand, it has been described the potential of the SSAO metabolic products to induce Aβ aggregation [35,99]. Besides the clear contribution of SSAO/VAP-1 to the AβD deposition, the increased expression of LRP-1 in hSSAO/VAP-1-expressing cells, which binds Aβ, could also contribute to the enhanced Aβ deposition on these cells. In this regard, the results presented in this work seem to be in controversy with the general observation of the LRP-1 decrease found in AD tissue, including ours [98]. The main hypothesis on the LRP-1 role in AD is based on the fact that the LRP-1 decrease promotes Aβ accumulation, initiating therefore the pathology. However, other

authors have found LRP-1 increased (reviewed in [100]), and interestingly, Sagare and collegues [101] observed an increase of oxidized sLRP-1 in the plasma of MCI individuals, which showed low affinity for Aβ, suggesting an impairment of Aβ clearance from the brain at this early stage of AD. In this context, we have observed the SSAO/VAP-1 increase and LRP-1 decrease in AD tissue when Aβ is already deposited on blood vessels, but it is not known what occurs before this point with these two proteins. Considering our in vitro model, we do not have an established AD situation, because our initiating point is only an increased SSAO/VAP-1 expression, so it is not surprising that we do not observe an LRP-1 decrease; by contrast, the LRP-1 increase may be due to other stimulus in our model, and could also be related to the BBB breakdown observed, an LRP-1 role suggested by others [102,103]. Similarly, we previously observed a RAGE increase in human AD tissue, while we do not observe changes in our in vitro model; in this sense, others and us hypothesize that this increase could be attributed to the increased AGEs levels detected in these patients, which is not present in our cell culture model. Obviously, the use of this or other models has limitations, because they are not able to consider all the players involved in the pathological process. In addition, AD is a multifactorial disease with probably several deregulations acting at the same time, and the molecular changes responsible of the initiation of the pathology, before the initial Aβ aggregation, are not fully understood yet. Thus, we are testing the SSAO/VAP-1 increase, which can be present in any inflammatory condition, as one of the alterations leading to the AD initiation and progression. In this regard, our model can be useful for this objective, although it may not consider other molecular players, as other models do not consider SSAO/VAP-1.

A slight increase in SSAO activity was observed after treating cells with AβD, indicating a crosstalk between these two molecules. This relationship was also evidenced at the BBB functional level, since results obtained after treatments with AβD and SSAO substrates and/or inhibitors revealed that SSAO/VAP-1 presence amplifies the effect of AβD on the BBB dysfunction, clearly affecting its permeability. The additive toxicity of AβD and MA treatments was also evidenced by the cell viability tests. However, the enzymatic SSAO activity is more related to the leukocyte adhesion process, with a small additive effect of the AβD treatment but a clear reduction in leukocyte adhesion in the presence of SSAO specific inhibitors.

In some of the parameters previously analyzed we did not obtain the same responses using AβD or $A\beta_{42}$. For instance, $A\beta_{\square\square}$ deposition was less modulated by SSAO/VAP-1 than AβD, changes in SSAO activity and cell viability were induced at lower $A\beta_{42}$ concentrations than AβD, and the cell death induced by $A\beta_{42}$ and MA was dependent on the mitochondrial apoptotic pathway while it was not by AβD and MA. We think that these differential effects could be related to the higher deposition rate of $A\beta_{42}$ (3 times higher than AβD according to our western blot experiments), which does not allow a modulation of its deposition procedure while the slower AβD aggregation rate does.

**5. Conclusions**

Our results indicate that the presence of SSAO/VAP-1 in human brain microvessels induces an endothelial activation status towards a pro-inflammatory phenotype, accompanied by BBB leakage and leukocyte adhesion. The molecular mechanisms regulating these phenotypic changes are not known, but they could be related to the activation of signaling pathways by the products generated during SSAO enzymatic activity or by structural modifications provoked by the SSAO/VAP-1 presence. Leukocyte adhesion and AβD deposition on endothelial cells are enhanced by SSAO enzymatic activity, indicating that SSAO/VAP-1 inhibition could report beneficial effects in the treatment of the AD progression. However, SSAO/VAP-1 also affects leukocyte adhesion, AβD deposition, as well as BBB permeability, by enzymatic activity-independent mechanisms. The pro inflammatory molecules over released by cells expressing hSSAO/VAP-1 could have consequences in the surrounding microenvironment, therefore affecting other neighboring cells in the brain and thus, the neurovascular unit function. These aspects should be evaluated in further experiments in order to determine the scope of these alterations in neurons and glia under AD conditions, where SSAO/VAP-1 is overexpressed.

**Funding**

This work was supported by grants from Ministerio de Economía y Competitividad (SAF2014-59697-R, SAF2017-89271-R), CIBERNED (CB06/05/0042), Fundació La Marató de TV3 (2014-3610) and Generalitat de Catalunya (SGR2009-1231 and SGR2014-0984). CF is supported by a grant from the Departament de Bioquímica i Biologia Molecular, in UAB.

**Acknowledgements**

We gratefully acknowledge Dr. Couraud (Institut Cochin, Paris, France), Dr. Babette Weksler (Weill Cornell Medical College, New York, NY) and Dr. Ignacio Romero (Open University, Milton Keynes, UK) for kindly providing the hCMEC/D3 cell line. We thank Dr. W. E. Van Nostrand (Stony Brook University, Stony Brook, NY, USA) for his kind gift of the hybridoma cell line producing the mouse anti-APP 20.1 antibody. We also acknowledge Dr. D. Smith (Biotie Therapeutics, Turku, Finland) for providing the SSAO inhibitors BTT 2079 and BTT 2089. Our gratefulness is also to our collegues from the microscope and histology facilities in the Institut de Neurociències of Universitat Autònoma de Barcelona (Barcelona, Spain).

**Author's contributions**

MS, MEL, BT, CF and AJMM performed the experiments. MS, AJMM and MU designed the experiments. MS and MU supervised the experiments and were responsible for writing the manuscript. RF, AJMM, NC and JRA contributed to the project design and manuscript writing. MU and JRA provided funding.

**Declaration of conflicting interests**

The authors declare no competing financial interests

**References**

1. BV. Zlokovic. Neurovascular pathways to neurodegeneration in Alzheimer's disease and other disorders. Nat Rev Neurosci 12 (2011) 723-738.
2. P. Grammas. Neurovascular dysfunction, inflammation and endothelial activation: implications for the pathogenesis of Alzheimer's disease. J Neuroinflammation 8 (2011) 26.
3. HM. Snyder, RA. Corriveau, S. Craft, JE. Faber, SM. Greenberg, D. Knopman, BT. Lamb, TJ. Montine, M. Nedergaard, CB. Schaffer, JA. Schneider, C. Wellington, DM. Wilcock, GJ. Zipfel, Zlolovic B, LJ. Bain, F. Bosetti, ZS. Galis, W. Koroshetz, MC. Carrillo. Vascular contributions to cognitive impairment and dementia including Alzheimer's disease. Alzheimers Dement 11 (2015) 710-717.

4. RF. Gottesman, AL. Schneider, Y. Zhou, J. Coresh, E. Green, N. Gupta, DS. Knopman, A. Minz, A. Rahmim, AR. Sharrett, LE. Wagenknecht, DF. Wong, TH. Mosley. Association between midlife vascular risk factors and estimated brain amyloid deposition. JAMA 317 (2017) 1443-1450.
5. C. Iadecola. The neurovascular unit coming of age: a journey through neurovascular coupling in health and disease. Neuron 96 (2017) 17-42.
6. MD. Sweeney, Z. Zhao, A. Montagne, AR. Nelson, BV Zlokovic. Blood-brain barrier: from physiology to disease and back. Physiol Rev 99 (2019) 21-78.
7. J. Zhou, JT. Yu, HF. Wang, XF. Meng, CC. Tan, J. Wang, C. Wang, L. Tan. Association between stroke and Alzheimer's disease: systematic review and meta-analysis. J Alzheimers Dis 43 (2015) 479-489.
8. A. Montagne, SR. Barnes, MD. Sweeney, MR. Halliday, AP. Sagare, Z. Shao, AW. Toga, RE. Jacobs, CY. Liu, L. Amezcua, MG. Harrington, HC. Chui, M. Law, BV. Zlokovic. Blood-brain barrier breakdown in the aging human hippocampus. Neuron 85 (2015) 296-302.
9. C. Peers, ML. Dallas, HE. Boycott, JL. Scragg, HA. Pearson, JP. Boyle. Hypoxia and neurodegeneration. Ann N Y Acad Sci 1177 (2009) 169-177.
10. AH. Vagnucc Jr, WW. Li. Alzheimer's disease and angiogenesis. Lancet 361 (2003) 605-608.
11. L. Thirumangalakudi, PG. Samany, A. Owoso, B. Wiskar, P. Grammas. Angiogenic proteins are expressed by brain blood vessels in Alzheimer's disease. J Alzheimers Dis 10 (2006) 111-118.
12. C. Schultheiss, B. Blechert, FC. Gaertner, E. Drecoll, J. Mueller, GF. Weber, A. Drzezga, M. Essler. In vivo characterization of endothelial cell activation in a transgenic mouse model of Alzheimer's disease. Angiogenesis 9 (2006) 59-65.
13. P. Grammas, R. Ovase. Inflammatory factors are elevated in brain microvessels in Alzheimer's disease. Neurobiol Aging 22 (2001) 837-842.
14. S. Zacchigna, D. Lambrechts, P. Carmeliet. Neurovascular signalling defects in neurodegeneration. Nat Rev Neurosci 9 (2008) 169-181.

15. P. Grammas, J. Martinez, A. Sanchez, X. Yin, J. Riley, D. Gay, K. Desobry, D. Tripathy, J. Luo, M. Evola, A. Young. A new paradigm for the treatment of Alzheimer's disease: targeting vascular activation. J Alzheimers Dis 40 (2014) 619-630.
16. C. Iadecola. The overlap between neurodegenerative and vascular factors in the pathogenesis of dementia. Acta Neuropathol 120 (2010) 287-296.
17. M. Ujiie, DL. Dickstein, DA. Carlow, WA. Jefferies. Blood-brain barrier permeability precedes senile plaque formation in an Alzheimer's disease model. Microcirculation 10 (2003) 463-470.
18. A. Montagne, Z. Zhao, BV. Zlokovic. Alzheimer's disease: A matter of blood-brain barrier dysfunction? J Exp Med 214 (2017) 3151-3169.
19. S. Takeda, N. Sato, D. Takeuchi, H. Kurinami, M. Shinohara, K. Niisato, M. Kano, T. Ogihara, H. Rakugi, R. Morishita. Angiotensin receptor blocker prevented beta-amyloid-induced cognitive impairment associated with recovery of neurovascular coupling. Hypertension 54 (2009) 1345-1352.
20. G. Aliev, MA. Smith, D. Sevdov, ML. Neal, BT. Lamb, A. Nunomura, EK. Gasimov, HV. Vinters, G. Perry, JC. LaManna, RP. Friedland. The role of oxidative stress in the pathophysiology of cerebrovascular lesions in Alzheimer's disease. Brain Pathol 12 (2002) 21-35.
21. S. Takeda, N. Sato, K. Ikimura, H. Nishino, H. Rakugi, R. Morishita. Increased blood-brain barrier vulnerability to systemic inflammation in an Alzheimer disease mouse model. Neurobiol Aging 34 (2013) 2064-2070.
22. BI. Rini. Sunitinib. Expert Opin Pharmacother 8 (2007) 2359-2369.
23. I. Ferrer, JM. Lizcano, M. Hernández, M. Unzeta. Overexpression of semicarbazide sensitive amine oxidase in the cerebral blood vessels in patients with Alzheimer's disease and cerebral autosomal dominant arteriopathy with subcortical infarcts and leukoencephalopathy. Neurosci Lett 321 (2002) 21-24.
24. M. del Mar Hernandez, M. Esteban, P. Szabo, M. Boada, M. Unzeta. Human plasma semicarbazide sensitive amine oxidase (SSAO), beta-amyloid protein and aging. Neurosci Lett 384 (2005) 183-187.

25. L. Airas, PJ. Lindsberg, ML. Karjalainen-Lindsberg, I. Mononen, K. Kotisaari, DJ. Smith, S. Jalkanen. Vascular adhesion protein-1 in human ischaemic stroke. Neuropathol Appl Neurobiol 34 (2008) 394-402.

26. M. Hernandez-Guillamon, L. Garcia-Bonilla, M. Solé, V. Sosti, M. Parés, M. Campos, A. Ortega-Aznar, C. Domínguez, M. Rubiera, M. Ribó, M. Quintana, CA. Molina, J. Álvarez-Sabín, A. Rosell, M. Unzeta, J. Montaner. Plasma VAP-1/SSAO activity predicts intracranial hemorrhages and adverse neurological outcome after tissue plasminogen activator treatment in stroke. Stroke 41 (2010) 1528-1535.

27. M. Hernandez-Guillamon, M. Solé, P. Delgado, L. García-Bonilla, D. Giralt, C. Boada, A. Penalba, S. García, A. Flores, M. Ribó, J. Álvarez-Sabín, A. Ortega-Aznar, M. Unzeta, J. Montaner. VAP-1/SSAO plasma activity and brain expression in human hemorrhagic stroke. Cerebrovasc Dis 33: (2012) 55-63.

28. R. Kurkijärvi, DH. Adams, R. Leino, T. Möttönen, S. Jalkanen, M. Salmi. Circulating form of human vascular adhesion protein-1 (VAP-1): increased serum levels in inflammatory liver diseases. J Immunol 161 (1998) 1549-1557.

29. F. Boomsma, UM. Bhaggoe, AM. van der Houwen, AH. van den Meiracker. Plasma semicarbazide-sensitive amine oxidase in human (patho)physiology. Biochim Biophys Acta 1647 (2003) 48-54.

30. R. Pannecoeck, D. Serruys, L. Benmeridja, JR. Delanghe, N. van Geel, R. Speeckaert, MM. Speeckaert. Vascular adhesion protein-1: Role in human pathology and application as a biomarker. Crit Rev Clin Lab Sci 52 (2015) 284-300.

31. PH. Yu, YL. Deng. Endogenous formaldehyde as a potential factor of vulnerability of atherosclerosis: involvement of semicarbazide-sensitive amine oxidase-mediated methylamine turnover. Atherosclerosis 140 (1998) 357-363.

32. M. Solé, M. Hernandez-Guillamon, M. Boada, M. Unzeta. p53 phosphorylation is involved in vascular cell death induced by the catalytic activity of membrane-bound SSAO/VAP-1. Biochim Biophys Acta 1783 (2008) 1085-1094.

33. S. Jalkanen, M. Karikoski, N. Mercier, K. Koskinen, T. Henttinen, K. Elima, K. Salmivirta, M. Salmi. The oxidase activity of vascular adhesion protein-1 (VAP-1)

induces endothelial E- and P-selectins and leukocyte binding. Blood 110 (2007) 1864-1870.

34. PF. Lalor, PJ. Sun, CJ. Weston, A. Martin-Santos, MJ. Wakelam, DH. Adams. Activation of vascular adhesion protein-1 on liver endothelium results in an NF-kappaB-dependent increase in lymphocyte adhesion, Hepatology 45 (2007) 465-474.
35. K. Chen, J. Maley, PH. Yu. Potential implications of endogenous aldehydes in beta-amyloid misfolding, oligomerization and fibrillogenesis. J Neurochem 99 (2006) 1413-1424.
36. M. Solé, AJ. Miñano-Molina, M. Unzeta. A cross-talk between Aβ and endothelial SSAO/VAP-1 accelerates vascular damage and Aβ aggregation related to CAA-AD. Neurobiol Aging 36 (2015) 762-775.
37. DJ. Smith, M. Salmi, P. Bono, J. Hellman, T. Leu, S. Jalkanen. Cloning of vascular adhesion protein 1 reveals a novel multifunctional adhesion molecule. J Exp Med 188 (1998) 17-27.
38. S. Jalkanen, M. Salmi. VAP-1 and CD73, endothelial cell surface enzymes in leukocyte extravasation. Arterioscler Thromb Vasc Biol 28 (2008) 18-26.
39. BB. Weksler, EA. Subileau, N. Perrier, P. Charneau, K. Holloway, M. Leveque, H. Tricoire-Leignel, A. Nicotra, S. Bourdoulous, P. Turowski, DK. Male, F. Roux, J. Greenwood, IA. Romero, PO. Couraud. Blood-brain barrier-specific properties of a human adult brain endothelial cell line. FASEB J 19 (2005) 1872-1874.
40. B. Weksler, IA. Romero, PO. Couraud. The hCMEC/D3 cell line as a model of the human blood brain barrier. Fluids Barriers CNS 10 (2013) 16.
41. P. Sun, G. Esteban, T. Inokuchi, J. Marco-Contelles, BB. Weksler, IA. Romero, PO. Couraud, M. Unzeta, M. Solé. Protective effect of the multitarget compound DPH-4 on human SSAO/VAP-1-expressing hCMEC/D3 cells under oxygen–glucose deprivation conditions: an *in vitro* experimental model of cerebral ischaemia. Br J Pharmacol 172 (2015) 5390-5402.
42. HJ. Ball, B. McParland, C. Driussi, NH. Hunt. Isolating vessels from the mouse brain using laser capture microdissection. Brain Res Brain Res Protoc 9 (2002) 206-113.

43. C. Malagelada, X. Xifro, A. Miñano, J. Sabria, J. Rodriguez-Alvarez. Contribution of caspase-mediated apoptosis to the cell death caused by oxygen-glucose deprivation in cortical cell cultures. Neurobiol Dis 20 (2005) 27-37.

44. J. Wiltfang, A. Smirnov, B. Schnierstein, G. Kelemen, U. Matthies, HW. Klafki, M. Staufenbiel, G. Hüther, E. Rüther, J. Kornhuber. Improved electrophoretic separation and immunoblotting of beta-amyloid (A beta) peptides 1-40, 1-42, and 1-43. Electrophoresis 18 (1997) 527-532.

45. JM. Lizcano, KF. Tipton, M. Unzeta. Purification and characterization of membrane-bound semicarbazide-sensitive amine oxidase (SSAO) from bovine lung. Biochem J 331 (1998) 69-78.

46. M. Unzeta, M. Solé, M. Boada, M. Hernández. Semicarbazide-sensitive amine oxidase (SSAO) and its possible contribution to vascular damage in Alzheimer's disease. J Neural Transm 114 (2007) 857-862.

47. L. Olson, C. Humpel. Growth factors and cytokines/chemokines as surrogate biomarkers in cerebrospinal fluid and blood for diagnosing Alzheimer's disease and mild cognitive impairment. Exp Gerontol 45 (2010) 41-46.

48. P. Carmeliet, C. Ruiz de Almodovar. VEGF ligands and receptors: implications in neurodevelopment and neurodegeneration. Cell Mol Life Sci 70 (2013) 1763-1778.

49. KP. Doyle, E. Cekanaviciute, LE. Mamer, MS. Buckwalter. TGFb signaling in the brain increases with aging and signals to astrocytes and innate immune cells in the weeks after stroke. J Neuroinflam 7 (2010) 62.

50. A. Fuster-Matanzo, M. Llorens-Martín, F. Hernández, J. Avila. Role of neuroinflammation in adult neurogenesis and Alzheimer's disease: Therapeutic approaches. Mediators Inflamm (2013) 1-9.

51. HS. Suh, ML. Zhao, L. Derico, N. Choi, SC. Lee. Insulin-like growth factor 1 and 2 (IGF1, IGF2) expression in human microglia: differential regulation by inflammatory mediators. J Neuroinflam 10 (2013) 37.

52. LA. Bach. Endothelial cells and the IGF system. J Mol Endocrinol 54 (2015) R1-13.

53. M. Erta, A. Quintana, J. Hidalgo. Interleukin-6, a major cytokine in the central nervous system. Int J Biol Sci 8 (2012) 1254-1266.

54. ML. Petreaca, M. Yao, Y. Liu, K. Defea, M. Martins-Green. Transactivation of vascular endothelial growth factor receptor-2 by interleukin-8 (IL-8/CXCL8) is required for IL-8/CXCL8-induced endothelial permeability. Mol Biol Cell 18 (2007) 5014-5023.

55. SS. Shaftel, WS. Griffin, MK. O'Banion. The role of interleukin-1 in neuroinflammation and Alzheimer disease: an evolving perspective. J Neuroinflamm 5 (2008) 7.

56. SJ. Lee, K. Drabik, NJ. Van Wagoner, S. Lee, C. Choi, Y. Dong, EN. Benveniste. ICAM-1-induced expression of proinflammatory cytokines in astrocytes: involvement of extracellular signal-regulated kinase and p38 mitogen-activated protein kinase pathways. J Immunol 165 (2000) 4658-4666.

57. P. Turowski, P. Adamson, J. Greenwood. Pharmacological targeting of ICAM-1 signaling in brain endothelial cells: potential for treating neuroinflammation. Cell Mol Neurobiol 25 (2005) 153-170.

58. M. Ewers, MM. Mielke, H. Hampel. Blood-based biomarkers of microvascular pathology in Alzheimer's disease. Exp Geront 45 (2010) 75-79.

59. BA. Kallmann, V. Hummel, T. Lindenlaub, K. Ruprecht, KV. Toyka, P. Rieckmann. Cytokine-induced modulation of cellular adhesion to human cerebral endothelial cells is mediated by soluble vascular cell adhesion molecule-1. Brain 123 (2000) 687-697.

60. A. Haarmann, E. Nowak, A. Deib, S. van der Pol, CM. Monoranu, G. Kooij, N. Müller, P. van der Valk, G. Stoll, HE. De Vries, F. Berberich-Siebelt. M. Buttamann. Soluble VCAM-1 impairs human brain endothelial barrier integrity via integrin a-4-transduced outside-in signaling. Acta Neuropathol 129 (2015) 639-652.

61. G. Zuliani, M. Cavalieri, M. Galvani, A. Passaro, MR. Munari, C. Bosi, A. Zurlo, R. Fellin. Markers of endotelial dysfunction in older subjects with late onset Alzheimer's disease or vascular dementia. J Neurol Sci 272 (2008) 164-170.

62. R. Deane, Z. Wu, A. Sagare, J. Davis, S. Du Yan, K. Hamm, F. Xu, M. Parisi, B. LaRue, HW. Hu, P. Spijkers, H. Guo, X. Song, PJ. Lenting, WE. Van Nostrand, BV Zlokovic. LRP/amyloid beta-peptide interaction mediates differential brain efflux of Abeta isoforms. Neuron 43 (2004) 333-344.

63. Y. Zhao, D. Li, J. Zhao, J. Song, Y. Zhao. The role of the low-density lipoprotein receptor-related protein 1 (LRP-1) in regulating blood-brain barrier integrity. Rev Neurosci 27 (2016) 623-634.

64. X. Wang, SR. Lee, K. Arai, SR. Lee, K. Truji, GW. Rebeck, EH. Lo. Lipoprotein receptor-mediated induction of matrix metalloproteinase by tissue plasminogen activator. Nat Med 9 (2003) 1313-1317.

65. U. Beffert, PC. Stolt, J. Herz. Functions of lipoprotein receptors in neurons. J Lipid Res 45 (2004) 403-409.

66. Z. Qiu, DK. Strickland, BT. Hyman, GW. Rebeck. Alpha 2-macroglobulin exposure reduces calcium responses to N-methyl-D-aspartate via low density lipoprotein receptor-related protein in cultured hippocampal neurons. J Biol Chem 277 (2002) 14458-14466.

67. T. Kanekiyo, JR. Cirrito, CC. Liu, M. Shinohara, J. Li, DR. Schuler, M. Shinohara, DM. Holtzman, G. Bu. Neuronal clearance of amyloid-b by endocytic receptor LRP-1. J Neurosci 33 (2013) 19276-19283.

68. M. Shinohara, M. Tachibana, T. Kanekiyo, G. Bu. Role of LRP1 in the pathogenesis of Alzheimer's disease: evidence from clinical and preclinical studies. J Lipid Res 58 (2017) 1267-1281.

69. Z. Cai, N. Liu, C. Wang, B. Qin, Y. Zhou, M. Xiao, L. Chang, LJ. Yan, B. Zhao. Role of RAGE in Alzheimer's Disease. Cell Mol Neurobiol 36 (2016) 483-495.

70. D. Walker, LF. Lue, G. Paul, A. Patel, MN. Sabbagh. Receptor for advanced glycation endproduct modulators: a new therapeutic target in Alzheimer's disease. Expert Opin Invest Drugs 24 (2015) 393-399.

71. R. Deane, S. Du Yan, RK. Submamaryan, B. LaRue, S. Jovanovic, E. Hogg, D. Welch, L. Manness, C. Lin, J. Yu, H. Zhu, J. Ghiso, B. Frangione, A. Stern, AM. Schmidt, DL. Armstrong, B. Arnold, B. Liliensiek, P. Nawroth, F. Hofman, M. Kindy, D. Stern, B. Zlokovic. RAGE mediates amyloid-beta peptide transport across the blood-brain barrier and accumulation in brain. Nat Med 9 (2003) 907-913.

72. O. Arancio, HP. Zhang, X. Chen, C. Lin, F. Trinchese, D. Puzzo, S. Liu, A. Hegde, SF. Yan, A. Stem, JS. Luddy, LF. Lue, DG. Walker, A. Roher, M. Buttini, L. Mucke, W. Li,

AM. Schmidt, M. Kindy, PA. Hyslop, DM. Stern, SS. Du Yan. RAGE potentiates Abeta-induced perturbation of neuronal function in transgenic mice. EMBO J 23 (2004) 4096-4105.

73. HH. Birdsall, C. Lane, MN. Ramser, DC. Anderson. Induction of VCAM-1 and ICAM-1 on human neural cells and mechanisms of mononuclear leukocyte adherence. J Immunol 148 (1992) 2717-2723.
74. E. Zenaro, G. Piacentino, G. Constantin. The blood-brain barrier in Alzheimer's disease. Neurobiol Dis 107 (2017) 41-56.
75. M. Dougher-Vermazen, JD. Hulmes, P. Böhlen, BI. Terman. Biological activity and phosphorylation sites of the bacterially expressed cytosolic domain of the KDR VEGF-receptor. Biochem Biophys Res Commun 205 (1994) 728-738.
76. Z. Sun, X. Li, S. Massena, S. Kutschera, N. Padhan, L. Gualandi, V. Sundvold-Gjerstad, K. Gustafsson, WW. Choy, G. Zhang, M. Quach, L. Jansson, M. Philipson, MR. Abid, A. Spurkland, L. Claesson-Welsh. VEGFR2 induces c-Src signaling and vascular permeability in vivo via the adaptor protein TSAd. J Exp Med 209 (2012) 1363-1377.
77. MC. Herzig, DT. Winkler, P. Burgermeister, M. Pfeifer, E. Kohler, SD. Schmidt, S. Danner, D. Abramowski, C. Struchler-Pierrat, K. Burki, SG. Van Duinen, ML. Maat-Shiemann, M. Staufenbiel, PM. Mathews, M. Jucker. Abeta is targeted to the vasculature in a mouse model of hereditary herebral hemorrhage with amyloidosis. Nat Neurosci 7 (2004) 954-960.
78. R. Natte, H. Yamaguchi, ML. Maat-Schieman, FA. Prins, P. Neeskens, RA. Roos, SG. van Duinen. Ultrastructural evidence of early non-fibrillar Abeta42 in the capillary basement membrane of patients with hereditary cerebral hemorrhage with amyloidosis, Dutch type. Acta Neuropathol 98 (1999) 577-582.
79. P. Carmeliet. Mechanisms of angiogenesis and arteriogenesis. Nat Med 6 (2000) 389-395.
80. SP. Yang, DG. Bae, HJ Kang, BJ. Gwag, YS. Gho, CB. Chae. Co-accumulation of vascular endothelial growth factor with beta-amyloid in the brain of patients with Alzheimer's disease. Neurobiol Aging 25 (2004) 283-290.

81. P. Grammas, R. Ovase. Cerebrovascular transforming growth factor-beta contributes to inflammation in the Alzheimer's disease brain. Am J Pathol 160 (2002) 1583-1587.
82. R. Schliebs, T. Arendt. The cholinergic System in aging and neuronal degeneration. Behav Brain Res 221 (2011) 555-63.
83. P. Podlesniy, A. Kichev, C. Pedraza, J. Saurat, M. Encinas, B. Perez, I. Ferrer, C. Espinet. Pro-NGF from Alzheimer's disease and normal human brain displays distinctive abilities to induce processin and nuclear translocation of intracellular domain of p75NTR and apoptosis. Am J Pathol 169 (2006) 119-131.
84. CJ. Xu, JL. Wang, WL. Jin. The emergint therapeutic role of NGF in Alzheimer's disease. Neurochem Res 41 (2016) 1211-1218.
85. XX. Wang, MS. Tan, JT. Yu, L. Tan. Matrix metalloproteinases and their multiple roles in Alzheimer's disease. Biomed Res Int (2014) 908636.
86. F. Yao, K. Zhang, Y. Zhang, Y. Guo, A. Li, S. Xiao, Q. Liu, L. Shen, J. Ni. Identification of blood biomarkers for Alzheimer's disease through compuntational prediction and experimental validation. Front Neurol 9 (2018) 1158.
87. P. Sun, M. Solé, M. Unzeta. Involvement of SSAO/VAP-1 in oxygen-glucose deprivation-mediated damage using the endothelial hSSAO/VAP-1-expressing cells as an experimental model of cerebral ischemia. Cerebrovascular Dis 37 (2014) 171-180.
88. BV. Zlokovic. Neurovascular mechanisms of Alzheimer's neurodegeneration. Trends Neurosci 28 (2005) 202-208.
89. N. Ahmed Khan, R. Siddiqui. The neuropathogenesis of Acanthamoeba encephalitis: Barriers to overcome. J Cell Sci Ther (2011) S3:001.
90. EE. Benarroch. Blood-brain barrier: recent developments and clinical correlations. Neurology 78 (2012) 1268-1276.
91. SJ. Cho, MH. Park, C. Han, K. Yoon, YH. Koh. VEGFR2 alteration in Alzheimer's disease. Sci Rep 7 (2017) 17713.
92. M. Zhang, L. Jiang. Oxidized low-density lipoprotein decreases VEGFR2 expression in HUVECs and impairs angiogenesis. Exp Ther Med 12 (2016) 3742-3748.

93. F. Jin, N. Hagemann, U. Brockmeier, ST. Schäfer, A. Zechariah, DM. Hermann. LDL attenuates VEGF-induced angiogènesis via mechanisms involving VEGFR2 internalization and degradation following endosome-trans-Golgi network trafficking. Angiogenesis 16 (2013) 625-637.

94. H. Liu, S. Yu, H. Zhang, J. Xu. Angiogenesis impairment in diabetis: role of methylglyoxal-induced receptor for advanced glycation endproducts, autophagy and vascular endothelial growth factor receptor 2. PLoS One 7 (2012) e46720.

95. W. Swardfager, K. Lanctôt, L. Rothenburg, A. Wong, J. Cappell, N. Herrmann. A meta-analysis of cytokines in Alzheimer's disease. Biol Psychiatry 68 (2010) 930-941.

96. SKL. Darweesh, FJ. Wolters, MA. Ikram, F. De Wolf, D. Bos, A. Hofman. Inflammatory markers and the risk of dementia and Alzheimer's disease: A meta-analysis. Alzheimers Dement (2018) S1552-5260 30068-2.

97. P. de Rossi, E. Harde, JP. Dupuis, L. Martin, N. Chounlamountri, M. Bardin, C. Watrin, C. Benetollo, K. Pernet-Gallay, HJ. Luhmann, J. Honnorat, G. Malleret, L. Groc, A. Acker-Palmer, PA. Salin, C. Meissirel. A critical role for VEGF and VEGFR2 in NMDA receptor synaptic function and fear-related behavior. Mol Psychiatry 21 (2016) 1768-1780.

98. T. Valente, A. Gella, M. Solé, N. Durany, M. Unzeta. Immunohistochemical study of semicarbazide-sensitive amine oxidase/vascular adhesion protein-1 in the hippocampal vasculature: pathological synergy of Alzheimer's disease and diabetes mellitus. J Neurosci Res 90 (2012) 1989-1996.

99. K. Chen, M. Kazachkov, PH. Yu. Effect of aldehydes derived from oxidative deamination and oxidative stress on beta-amyloid aggregation; pathological implications to Alzheimer's disease. J Neural Transm (Vienna) 114 (2007) 835-839.

100. M. Shinohara, M. Tachibana, T. Kanekiyo, G. Bu. Role of LRP1 in the pathogenesis of Alzheimer's disease: evidence from clinical and preclinical studies. Thematic review series: ApoE and Lipid Homeostasis in Alzheimer's disease, J Lipid Res 58 (2017) 1267-1281.

101. AP. Sagare, R. Deane, H. Zetterberg, A. Wallin, K. Blennow, BV. Zlokovic. Impaired lipoprotein receptor-mediated peripheral binding of plasma amyloid-β is an

early biomarker for mild cognitive impairment preceding Alzheimer's disease. J Alzheimers Dis 24 (2011) 25-34.

102. M. Yepes, M. Sandkvist, EG. Moore, TH. Bugge, DK. Strickland, DA. Lawrence. Tissue-type plasminogen activator induces opening of the blood-brain barrier via the LDL receptor-related protein. J Clin Invest 112 (2003) 1533-1540.

103. Y. Zhao, D. Li, J. Song, Y. Zhao. The role of the low-density lipoprotein receptor-related protein 1 (LRP-1 in regulating blood-brain barrier integrity. Rev Neurosci 27 (2016) 623-634.

HIGHLIGHTS

- SSAO/VAP-1 expression induces vascular endothelium activation
- An increased BBB permeability is associated to the SSAO/VAP-1 expression
- Angioneurins release by SSAO/VAP-1-expressing cells contributes to the BBB opening
- Secretion of IL-6 and STAT3 activation are involved in BBB permeability increase
- SSAO/VAP-1 expression and activity promote β-amyloid deposition and cytotoxicity